From THE DEPARTMENT OF DENTAL MEDICINE
Karolinska Institutet, Stockholm, Sweden

EVALUATION OF CONE BEAM COMPUTED TOMOGRAPHY WITH RESPECT TO EFFECTIVE RADIATION DOSE AND DIAGNOSTIC PROPERTIES

Nils Kadesjö

Karolinska Institutet

Stockholm 2020

Published by Karolinska Institutet.
Printed by Eprint AB, 2020

ISBN 978-91-7831-679-3

Evaluation of cone beam computed tomography with respect to effective radiation dose and diagnostic properties.
THESIS FOR DOCTORAL DEGREE (Ph.D.)

By

Nils Kadesjö

Principal Supervisor:
Professor Xie Qi Shi
University of Bergen
Faculty of Medicine
Department of Clinical Dentistry

Karolinska Institutet
Department of Dental Medicine
Division of Oral Diagnostik & Rehabilitering

Co-supervisor(s):
Professor Mats Nilsson
Skåne University Hospital
Department of Medical Radiation Physics

Odont Dr Karin Näsström
Malmö Universitet
Faculty of Odontology

Opponent:
Professor Hilde Bosmans
University of Leuven
Department of Imaging & Pathology
Division of Medical Physics & Quality Assessment

Examination Board:
Professor Ralf Schulze
Universität Mainz
Department of Oral and Maxillofacial Surgery
Division of Oral Radiography

Associate Professor Mikael Gunnarsson
Lunds Universitet
Department of Translationell Medicin
Division of Medicinsk strålningsfysik, Malmö

Associate Professor Agneta Karsten
Karolinska Institutet
Department of Dental Medicine
Division of Orthodontics and Pedodontics

ABSTRACT

Cone beam computed tomography (CBCT) is an x-ray modality providing three-dimensional x-ray images. CBCT devices have high resolution compared to traditional medical CT, making them suitable for examination of fine details. However, CBCT devices are worse at showing contrast differences, making them less suitable for examinations of soft tissue such as the brain and many other internal organs. An x-ray modality suitable for imaging of small details and hard tissue fits dental and maxillofacial radiology well. After the introduction of dentomaxillofacial CBCT in 1998, CBCT examinations have spread to become a common and important diagnostic tool in odontology. Today, CBCT examinations complement or replace examinations previously performed by other methods.

When choosing an x-ray imaging modality and examination parameters, concern must be taken for the diagnostic value and the radiation dose. The examination should be chosen to provide as low radiation dose as possible while not sacrificing the diagnostic value. In order to provide guidelines on the use of CBCT, scientific knowledge on CBCT and alternative examinations are needed. What is the radiation dose for different examinations and how does the examination affect diagnosis and treatment? This thesis aims to provide additional information in this field, to provide reference data when considering the choice of examination and the establishment of guidelines.

In the first paper, examinations of the temporomandibular joint, using CBCT and traditional medical multi-detector CT (MDCT), were compared to determine if CBCT examinations would result in lower radiation dose. The examinations were optimized to find the lowest suitable dose levels, and at these optimized dose levels no significant difference was found between CBCT and MDCT.

The second paper investigated the radiation dose from multiple different x-ray examinations of possible resorption impacted maxillary canines in children. CBCT examinations were compared to two-dimensional examinations using intraoral radiographs, and in some cases panoramic radiographs. CBCT examinations ranged from 15 to 140 times higher radiation dose, depending on x-ray device.

The third paper investigated the possibility of reducing the image size, and therefore the x-ray dose, in panoramic radiographs. A full-size panoramic radiograph was required in 20% of adult patient cases. The introduction of two different image sizes for adult patients would reduce the collective radiation dose from panoramic examinations by about 40% in our university clinic.

The fourth paper investigated radiation doses from different examinations and settings using the Newtom 5G CBCT device. This CBCT model use automatic exposure control and does not allow manual adjustment of exposure parameters. The resulting effective doses should be applicable to examinations of adult patients using this CBCT model.

LIST OF SCIENTIFIC PAPERS

I. Kadesjö N, Benchimol D, Falahat B, Näsström K, Shi X-Q. Evaluation of the effective dose of cone beam CT and multislice CT for temporomandibular joint examinations at optimized exposure levels. Dentomaxillofacial Radiol. 2015;44(8).

II. Kadesjö N, Lynds R, Nilsson M, Shi X-Q. Radiation dose from X-ray examinations of impacted canines: cone beam CT vs two-dimensional imaging. Dentomaxillofacial Radiol. 2018;47(7).

III. Benchimol D, Koivisto J, Kadesjö N, Shi XQ. Effective dose reduction using collimation function in digital panoramic radiography and possible clinical implications in dentistry. Dentomaxillofacial Radiol. 2018;47(7).

IV. Kadesjö N, Koivisto J, Shi X-Q. Effective dose from the different dental and temporomandibular joint protocols available for the NewTom5G cone-beam CT scanner. Manuscript.

CONTENTS

1 Introduction 1
1.1 Purpose 1
1.2 What is CBCT? 2
1.2.1 What is the difference between CBCT and “regular” CT? 2
1.2.2 The effect of different examination parameters 3
1.3 Dosimetry 6
1.3.1 Dosimetric quantities 6
1.3.2 Organ dosimetry 9
2 Study specific aims 11
3 Methods and materials 13
3.1 X-ray devices and phantoms 13
3.1.1 Study I 13
3.1.2 Study II 13
3.1.3 Study III 13
3.1.4 Study IV 13
3.2 Applied dosimetry (Study I-IV) 14
3.3 Radiation detectors and callibration (Study I-IV) 15
3.3.1 Uncertainty estimates 15
3.3.2 Thermoluminescent dosimeters 17
3.3.3 Dosimetric film 17
3.3.4 MOSFET dosimeters 17
3.3.5 DAP measurements 18
3.4 Optimization of dose and image quality (Study I & III) 18
3.4.1 Exposure level (study I) 18
3.4.2 Image size (study III) 19
4 Study Results and discussions 21
4.1 Study I 21
4.1.1 Results 21
4.1.2 Discussion 23
4.2 Study II 25
4.2.1 Results 25
4.2.2 Discussion 25
4.3 Study III 26
4.3.1 Results 26
4.3.2 Discussion 28
4.4 Study IV 30
4.4.1 Results 30
4.4.2 Discussion 31
5 Study conclusions 33
5.1 Study I 33
5.2 Study II 33

5.3 Study III 33
5.4 Study IV 34
6 General discussions 35
6.1 Generalisation 35
6.1.1 Uncertainties in patient dosimetry 35
6.1.2 Effective dose conversion factors 36
7 General conclusions and future aspects 39
8 Acknowledgements 41
9 References 43
10 Errata 47
10.1 Study III 47

ABBREVIATIONS AND GLOSSARY

CBCT	Cone-beam computed tomography
CNR	Contrast-to-noise ratio
CT	Computed tomography
CTDI	Computed tomography dose index
CsI	Cesium iodine
D	Absorbed dose, unit Gy.
DAP	Dose-area product
DLP	Dose-length product
DVT	Digital volumetric tomography. A synonym for dentomaxillofacial CBCT.
E	Effective dose
FOV	Field of view. Defined as diameter × height for CBCT.
Gy	Gray. J/kg Unit for kerma and for absorbed dose.
H_t	Mean organ dose for tissue *t*
HVL	Half-value layer, a measure of energy in an x-ray spectrum.
ICRP	International commission on radiological protection
ICRU	International commission on radiation units and measurements
K	Kerma (Kinetic energy released in mater), unit Gy
mA	Milliampere, tube current
mAs	Milliampere-seconds, tube current-exposure time product
MDCT	Multi-detector computed tomography. Often used as a synonym for conventional medical CT in the literature, in contrast to CBCT.
MOSFET	Metal oxide semiconductor field effect transistor
MSCT	Multi-slice computed tomography. A synonym for MDCT. Often used as a synonym for conventional medical CT in the literature, in contrast to CBCT.
s	Experimentally determined standard deviation.
Sv	Sievert. Unit for effective dos and for equivalent dose.
TLD	Thermoluminescent dosimeter

TM50	Endosteum. Not the actual endosteum, but the radiological surrogate tissue representing the osteoprogenitor cells. Defined as a 50 μm layer inside the trabecular cavities and lining the medullary cavity.
TMJ	Temporomandibular joint
Type A uncertainty	Uncertainty determined statistically through repeated measurements.
Type B uncertainty	Uncertainty determined through different methods from type A.
w_t	Effective dose tissue weighting factor for tissue *t*

1 INTRODUCTION

1.1 PURPOSE

Dentomaxillofacial cone-beam computed tomography (CBCT), also called digital volumetric tomography (DVT), flat-detector CT or flat-panel CT, is a relatively new radiological modality. It was introduced in 1998 and has quickly grown to become common throughout dento-maxillofacial radiology, complementing or replacing other imaging modalities. With the introduction of a new x-ray modality the two basic principles of radiation protection must be considered: *justification* and *optimization*. In terms of radiology these concepts can be summarized as: "*When should we use CBCT?"* and "*How should we use CBCT?"*

In order to establish guidelines addressing these two basic questions, several aspects must be considered. In the case of *when*, the principal aspect is the diagnostic efficiency. How accurate is CBCT compare to other modalities on a given diagnostic task? And ultimately, how does this diagnostic information affect the choice of treatment? Other important considerations are radiation dose and economic cost; if several modalities provide sufficient diagnostic properties for the tasks at hand, the one providing the lowest radiation dose should be used. Additionally, within each radiological modality, there are aspects affecting the image quality/general diagnostic value and radiation dose. Therefore, in order to optimize the radiation dose, examination protocols should take the diagnostic need for the specific task and the specific patient into account. In addition, due to limited resources, the economic cost of an imaging modality must be considered.

To establish such evidence-based guidelines there is a need for a scientific knowledge base regarding the aspects mentioned above. What are the diagnostic, radiation dose and economic properties of CBCT and the alternative modalities for different examinations? It is in this field the current thesis acts, providing reference information where prior knowledge is lacking, with an emphasis on dosimetry.

When planning the work covered in this thesis, we have primarily looked at *Cone Beam CT for Dental and Maxillofacial Radiology: Evidence-based Guidelines* produced by the SEDENTEXCT project and published by the European Commission in 2012.[1]

1.2 WHAT IS CBCT?

CBCT is at its core a type of computed tomography, i.e., an x-ray imaging modality where several x-ray images are acquired from many angles around an object of interest, and from these 2D-projection images cross-sectional images are computed. Within medicine and odontology, this allows us to get a complete, non-overlapping, view into the patient without resorting to the scalpel. In contrast, conventional x-ray images are summation images, where all structures along the x-ray beam are shown overlapping, sometimes hiding abnormalities behind more distinct normal structures.

CBCT was first introduced in odontology by Mozzo et al. in 1998.[2] Since then, CBCT has quickly reached wide acceptance and adoption within dento-maxillofacial radiology. The adoption of CBCT has been slower within medical diagnostic radiology, but CBCT can today be found within interventional radiology, surgery, mammography and skeletal radiology as well as within radiotherapy. However, the x-ray imaging modality CBCT is, surprisingly, not obvious to define.

1.2.1 What is the difference between CBCT and "regular" CT?

To describe the difference between cone-beam CT and multi detector CT we must first define a number of technical terms. The size of the x-ray field in CT can be defined by the fan angle, in the plane of rotation, and the cone angle, perpendicular to the plane of rotation (Figure 1). Conventional medical CT (MDCT and earlier single detector row CT) use a small cone angle and larger fan angle, giving the x-ray field a "fan-like" shape. As compared to MDCT, CBCT generally uses a larger cone angle and smaller fan angle, giving the x-ray field a rectangular cone shape.

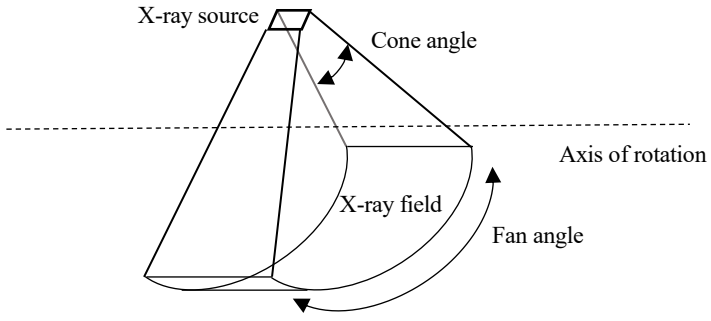

Figure 1 Fan angle and cone angle of a CT x-ray field.

Early CT reconstruction assumed parallel rays, which require low cone angles. With the introduction of MDCT with an increasing number of detector rows, the cone angles also increased. With increasing cone angles the assumption of parallel rays breaks down, requiring corrections such as the Feldkamp cone-beam algorithm.[3] Up to about four-detector-row MDCT images could be reconstructed without cone-beam correction, but all modern MDCT use cone-beam algorithms.[4]

Thus, it is not the cone angle that defines what is and is not called a CBCT device. The ICRP report on radiation protection in CBCT (ICRP 129) defines it as a CT with an area detector, acquiring a 3D volumetric image in one rotation.[5] In practice, this means that apart from a large cone angle and large z-coverage, we need a detector with a very small pixel pitch to provide sufficient z-resolution. In all modern CBCT this takes the shape of a flat-panel detector with a CsI scintillator, and it is this detector that gives CBCT most of its characteristics.

A flat-panel CsI detector allows for thick scintillation layers with minor reduction in resolution, thus maintaining relatively high sensitivity in high-resolution imaging. Compared to a MDCT detector array, a CBCT detector will allow higher spatial resolution. However, this comes at the price of image contrast. The CBCT detectors are not as sensitive as MDCT detectors and in addition, the smaller voxel sizes used in CBCT results in noisier images unless the radiation dose is increased to compensate. Another drawback with flat-panel detectors is that CsI is a relatively slow scintillator, requiring slower rotation times to avoid problems with detector afterglow. This, in turn, makes CBCT more prone to motion artifacts compared to MDCT.

In effect, we have in CBCT a CT modality suitable for imaging of small details and high-contrast objects such as bone or iodine contrast medium but unsuitable for low-contrast objects such as soft tissue. This makes CBCT excellent in dentistry with its high-contrast teeth and bone, and requirement to detect tiny lesions. Dental CBCT, in addition, often make use of volume-of-interest imaging, CT images with small radius limited to the object of interest, to reduce the x-ray field and thereby the radiation dose compared to MDCT.

1.2.2 The effect of different examination parameters

1.2.2.1 What do we want to see?

Two aspects affecting diagnostic image quality are spatial resolution, *how small objects can we see*, and contrast resolution, *how small contrast can we see.* The contrast resolution depends on the noise inside the x-ray image; if an object's contrast is small compared to the noise it will be hard or impossible to distinguish the object (Figure 2). The noise in an x-ray image will increase at a lower radiation dose. Thus, the radiation dose and image quality are intimately connected. Our diagnostic requirements will determine the dose level needed for the image.

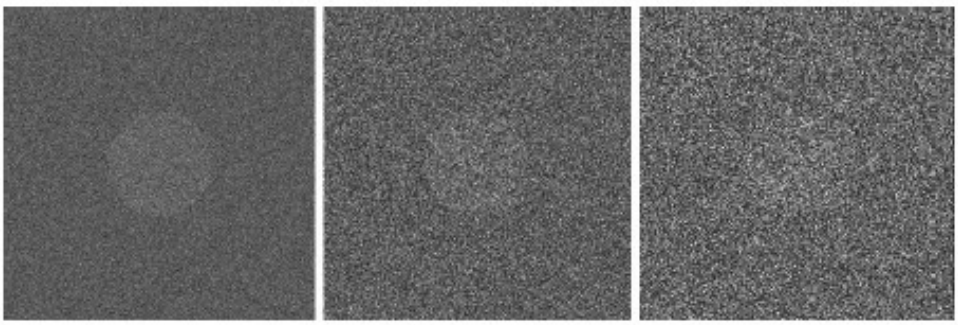

Figure 2 Three images with the same contrast but increasing levels of noise.
Image from: Diagnostic Radiology Physics: A Handbook for Teachers and Students. International atomic energy agency, 2014. © IAEA

1.2.2.2 X-ray tube parameters

The x-ray beam quality and radiation output are mostly determined by the following x-ray tube parameters: tube current-exposure time product (mAs), tube voltage (kV) and tube filtration.

Both tube current and exposure time are directly proportional to the radiation dose and are therefore commonly combined into mAs when described and in exposure settings. Depending on the x-ray modality one or both of these parameters can be adjusted, but the results in terms of dose are the same.

Tube voltage is the voltage between the cathode and anode inside the x-ray tube. This determines the maximum x-ray energy and affects the x-ray spectrum. The effect of tube voltage on radiation dose is more complex, but, all other parameters being equal, a higher tube voltage will result in a higher dose.

The tube filtration affects the shape of the x-ray spectrum. Additional filtration is added to reduce the low energy parts of the spectrum; higher filtration will generally reduce the dose but will disproportionally affect the lower energies, thus raising the mean energy of the spectrum (Figure 3).

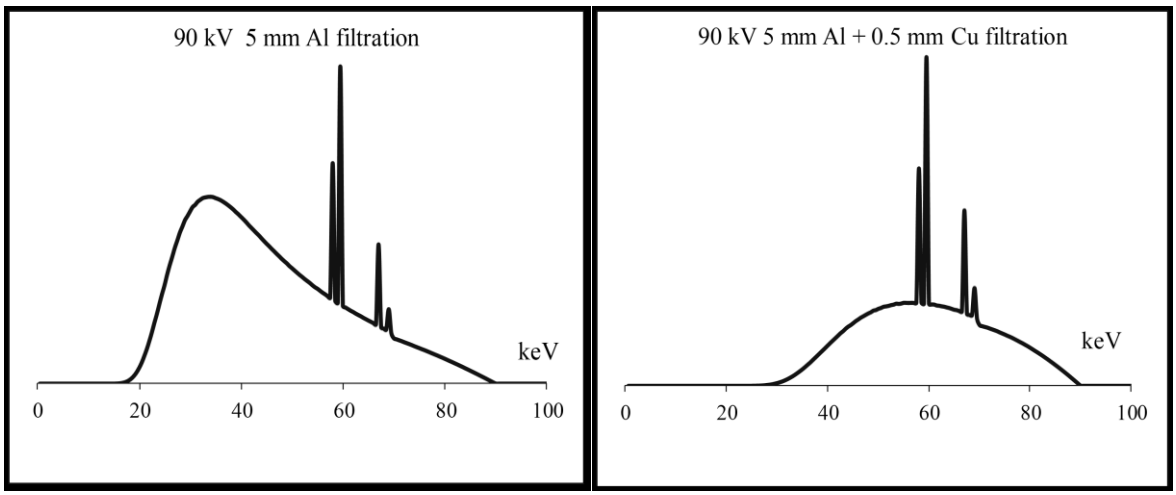

Figure 3 Simulated x-ray spectrum from an early version of the Promax3D CBCT without copper filtration compared to later spectra with copper filtration.

There are complex reasons for wanting a certain x-ray energy. At lower x-ray energy the contrast between different materials increases. Thus, it becomes easier to distinguish low-contrast variations in tissue, especially subtler differences as in soft tissues. However, low energies are also more likely to interact with matter and at too low energy almost all rays will be absorbed inside the patient, resulting in radiation dose with little portion contributing to the image. The optimal energy (in terms of image quality per patient dose) will vary due to the material and thickness of the examined objects/tissues, as well as the effectiveness of the image detector at different energies.

1.2.2.3 Voxel size, FOV and number of acquisition frames

Voxels (3D pixels) are the building blocks that make up the reconstructed CBCT volumes. Smaller voxels will increase the theoretical spatial resolution and allow higher frequencies, smaller details, to be displayed. Smaller voxels, however, comes at the cost of radiation dose or image noise. With a smaller voxel, fewer photons contribute to the signal in each voxel, resulting in a nosier image, unless the radiation dose is increased to compensate.

Small voxels will also require sufficient sampling of data, both ray-sampling by having sufficiently small detector pixel pitch and view-sampling by acquiring a sufficient number of image frames (or views) during the rotation.

Using smaller voxel sizes than the data sampling rates allow, in fan direction or cone direction, will result in artifacts. At small amounts of under-sampling these artifacts will not be as noticeable and might not adversely affect diagnostics; it is common for CT to operate bellow the required sampling rate.[6] However, the artifacts will become progressively worse with increased under-sampling.

Increasing the FOV will theoretically affect the image quality negatively in CBCT due to an increase of scattered radiation causing noise in the image. What's probably more important, however, is that an increase in FOV height results in an increased cone angle. This will negatively affect the resolution in parts of the reconstructed image where the x-ray beam

angle is higher. In practice, CBCT devices will often allow smaller voxel sizes when a smaller FOV is employed.

1.3 DOSIMETRY

The central element of dosimetry is that radiation dose is not measured directly. What we mean by "measuring dose" is that our radiation detectors measure one quantity, usually charge, and this is in turn related to a dosimetric quantity. The term *radiation dose* is, however, often haphazardly applied to many related but different quantities. Further increasing the complexity is the fact that dose is determined to specific materials; dose to air is not the same as dose to water, dose to lung tissue is a different quantity than dose to muscle.

1.3.1 Dosimetric quantities

1.3.1.1 Kerma and absorbed dose

Two basic concepts in dosimetry are kerma and absorbed dose. Kerma is defined as the energy transferred from uncharged particles (such as x-ray photons) to charged particles (such as electrons) inside a sample, divided by the mass of this sample. Absorbed dose is in turn defined as the energy imparted to a sample, divided by the mass. The concept is illustrated in Figure 4, where a photon (hν) interacts with the mass inside the volume (V) and transfers its energy to an electron (e^-). The distinction is that kerma does not account for any radiative losses carried by charged particles, in this case, energy carried outside the volume by electrons in the form of kinetic energy. Absorbed dose on the other hand only includes the energy imparted, i.e., the energy remaining inside the volume. In the special case where there are no radiative losses, absorbed dose is equal to kerma (Figure 5).

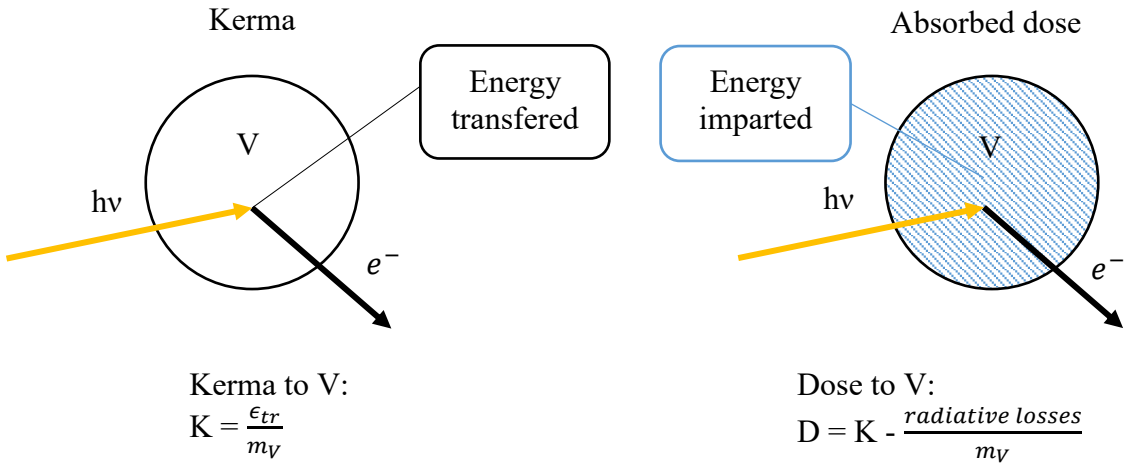

Figure 4 Illustration of the kerma and the absorbed dose inside the volume V, in the case of some energy leaving volume as kinetic energy.

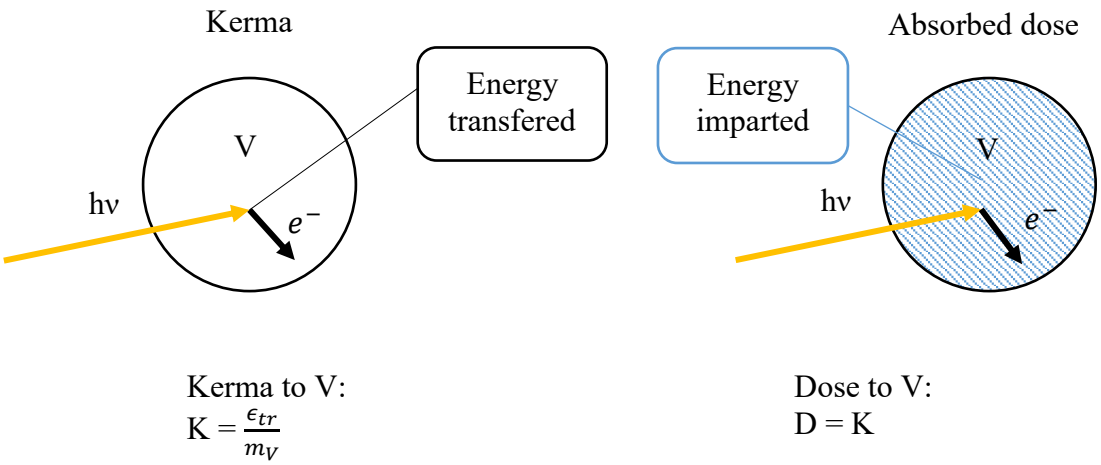

Figure 5 In the special case of no radiative losses, the absorbed dose becomes equal to the kerma.

In practice, the same conditions will be achieved if any energy leaving the volume carried by charged particles is matched by an equal addition from outside the volume, so-called charged particle equilibrium (CPE). In an x-ray field, assuming negligible photon attenuation over distances at the scale of the maximum range of the electrons, CPE will be achieved at the maximum electron range from any interfaces between different materials (Figure 6).

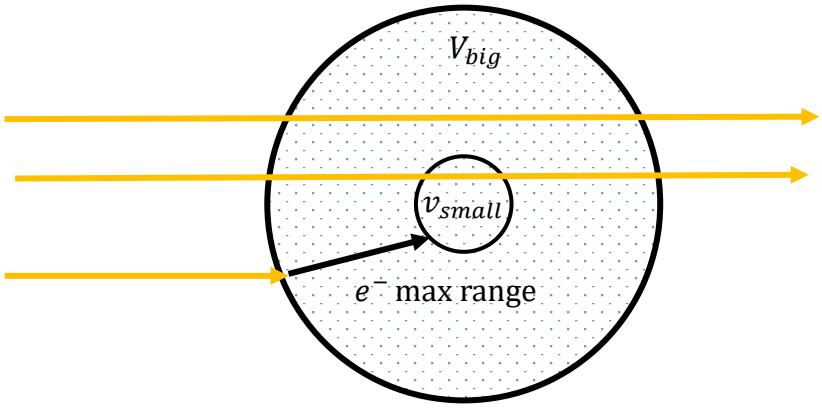

Figure 6 The volume V_{big} consists of homogenous matter, surrounded by another material. CPE will be achieved within the smaller volume v_{small}, defined by the maximum electron range.

This means that the absorbed dose and kerma will differ close to the interfaces between materials, with the difference gradually decreasing with distance from the interfaces (Figure 7). The range of these interface effects will increase with photon energy, with diagnostic x-ray energies resulting in about a hundred micrometer range.[7]

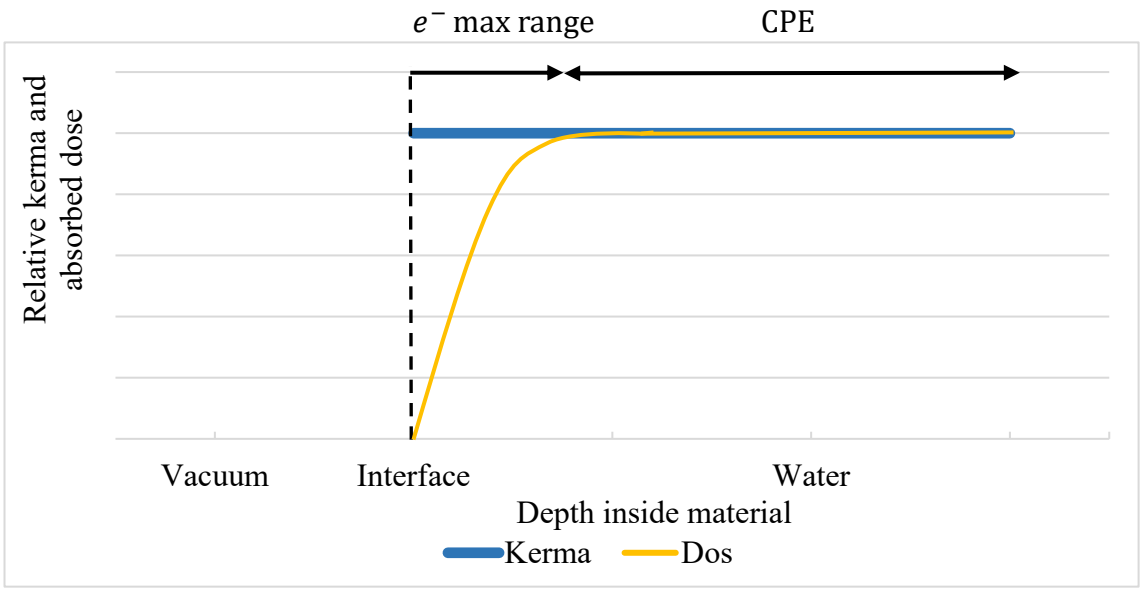

Figure 7 Relative difference between kerma and absorbed dose. Normalized to the kerma at the current depth in water.

The assumption of CPE is important in diagnostic x-ray dosimetry since it means that the absorbed dose is proportional to the mass-energy absorption coefficient of a material: $(\bar{\mu}_{en}/\rho)$. This allows us to convert dose to different materials by the mass-energy absorption coefficient ratio between the two materials: $(\bar{\mu}_{en}/\rho)_{mat1}^{mat2}$.

1.3.1.2 Effective dose

Absorbed dose is a purely physical concept and is limited in that it has no direct relation to the risk of radiation-induced harm. The concept of *effective dose* was introduced by the ICRP to compare delayed radiation risk from different kinds of irradiations of humans. Effective dose is defined as the sum of the mean organ dose for certain tissues at risk, multiplied by a weighting factor related to the relative "radiation sensitivity" of the tissue in question (Equation 1). The latest tissue weighting factors were published in IRCP 103 in 2007 (Table 1).[8]

$$E = \sum_t H_t \cdot w_t \qquad (1)$$

Table 1 Tissue weighting factors for effective dose.

Tissue	w_t
Red bone-marrow, Colon, Lung, Stomach, Breast	0.12 each
Gonads	0.08 each
Urinary bladder, Esophagus, Liver, Thyroid	0.04 each
Endosteum (Bone surface), Brain, Salivary glands, Skin	0.01 each
Remaining tissues: Adrenals, extrathoracic airways, gall bladder, heart, kidney, lymphatic nodes, muscle, oral mucosa, pancreas, prostate, small intestine, spleen, thymus, uterus	0.12 combined

It is essential to remember that effective dose is not defined for individuals, but for the entire population. Effective dose was introduced as a legal quantity to allow the setting of dose limits and to have a quantity to optimize when planning radiation protection.[8] It should never be quantify individual risk, or even quantify risk for subgroups of the population, such as specific age groups. There is also a lack of scientific evidence on how inhomogeneous irradiation of tissue, e.g. the active bone marrow during a head CT examination, will affect the radiation risk. However, even with all the disclaimers and uncertainties involved in effective dose it is still a useful tool when comparing different radiological examinations. "Effective dose can be of value for comparing doses from different diagnostic procedures and for comparing the use of similar technologies and procedures in different hospitals and countries as well as the use of different technologies for the same medical examination."[8] However, when comparing similar examinations of the same area, ICRP103 recommends the use of dose indexes instead of effective dose to avoid introducing unnecessary uncertainties.

1.3.1.3 Dose indexes

Dose indexes are defined to quantify the radiation output from an x-ray device in a way that is easy to measure. In the case of medical CT there are two important indexes *CTDI* and *DLP,* and in radiography, intervention, panoramic and CBCT there are *DAP*.[9]

DAP is defined as the mean air kerma inside the x-ray field, multiplied with the area of the x-ray field at the same distance (Figure 8). While the radiation dose will decrease with distance from the x-ray source due to geometric dispersion, the DAP will remain identical if the attenuation in air is negligible. Therefore, the DAP can easily be measured by a transmission ionization chamber placed at the x-ray tube side.

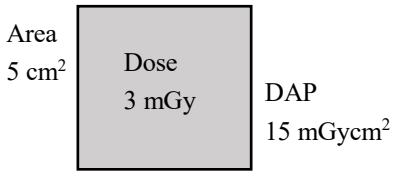

Figure 8 DAP is calculated from the product of the mean air kerma and the area of an x-ray field.

For these relatively easily measurable dose indexes, conversion factors to effective dose can be determined by measuring or simulating the effective dose under certain conditions and relating the dose index to effective dose under these conditions.[10]

1.3.2 Organ dosimetry

To determine the effective dose, the mean organ dose must be determined for the organs of interest, which presents two problems: determining the dose to the organ at certain points and estimating the mean dose through the organ from these sampling points.

The radiation detector will not be made of the same material as the organ tissue, thus the dose will need to be converted using appropriate conversion factors. In practice, theoretical radiological surrogate tissues, defined to estimate the properties of real organ tissue, will be

used, such as the ones defined by the International Commission on Radiation Units and Measurements.[9]

For most organs, CPE can be assumed at diagnostic energies; the tissue can be assumed to be reasonable homogenous on the 100 μm scale relevant for the interface effects. Thus, mass-energy absorption ratios, published for commonly used surrogate tissues, can be used to determine the dose.[11] However, the skeletal tissues are an exception; inside the trabecular bone the assumption of CPE breaks down due to a significant electron contribution from the bone into the marrow cavities, thus increasing the dose to the active marrow and the osteoprogenitor cells.[12]

2 STUDY SPECIFIC AIMS

Study I Would CBCT examinations of the temporomandibular joint reduce the effective dose as compared to MDCT examinations? (SEDENTEXCT 4.4.6)

Study II Determining the effective dose from CBCT examinations and from conventional 2D radiographic examinations on maxillary impacted canines.

Study III Determining the dose optimization potential of applying the segmentation (collimation) function in panoramic radiography and its possible clinical applications.

Study IV Determining the effective dose from the different dental examination protocols on the Newtom 5G CBCT device.

3 METHODS AND MATERIALS

3.1 X-RAY DEVICES AND PHANTOMS

3.1.1 Study I

Two x-ray devices were investigated, a Promax 3D (Planmeca Oy, Helsinki, Finland) CBCT and a Lightspeed VCT (GE healthcare, Chicago, USA) MDCT. The Promax 3D was operated at 90kV tube current (8.0 mm Al HVL) and the Lightspeed VCT was operated at 120kV (6.4 mm Al HVL).

Two anthropomorphic phantoms were used. Phantom 1, used for dosimetric measurements, was a sliced Alderson Rando dosimetric phantom consisting of a human dry skull inside tissue-equivalent plastic. Phantom 2, used for dose and image quality optimization, was a non-sliced phantom consisting of a human dry skull inside tissue-equivalent plastic.

61 measurement points were used throughout phantom 1, chosen to correspond to the organs expected to contribute the most to the effective dose. Two TLDs were positioned at each measurement point.

3.1.2 Study II

Four x-ray devices were investigated including two CBCTs, a Promax 3D operating at 90 kV (8.0 mm Al HVL) and a Newtom 5G (QR, Verona, Italy) operating at 110 kV (4.4 mm Al HVL), one panoramic x-ray: Promax 2D (Planmeca Oy) operating at 62 kV (2.9 mm Al HVL) and one intraoral x-ray: Prostyle Intra (Planmeca Oy) operating at 66 kV (2.1 mm Al HVL).

An anthropomorphic 10-year child phantom ATOM-706-C (CIRS, Norfolk, USA), made of tissue-equivalent plastic, was employed.

For TLD measurements on the CBCT devices 34 measurement points were used throughout the phantom. Two TLDs were positioned at each measurement point.

3.1.3 Study III

One panoramic x-ray device was investigated: Promax 2D (Planmeca Oy). All exposures were performed at 66 kV tube potential (3.4 mm Al HVL) and 8 mA tube current. One sliced anthropomorphic Alderson Rando phantom was used. 20 measurement points was used thought the phantom, with one MOSFET-detector placed at each point.

3.1.4 Study IV

One CBCT device was investigated Newtom 5G (QR) operating at 110 kV (4.4 mm Al HVL). One sliced anthropomorphic Alderson Rando phantom was used. 20 measurement points was used thought the phantom, with one MOSFET-detector placed at each point.

3.2 APPLIED DOSIMETRY (STUDY I-IV)

Effective dose was determined to allow dose comparison between different x-ray modalities. The effective dose was calculated according to ICRP 103.[8] Tissue weighting factors from ICRP 103 are shown in Table 1. For the 13 "remainder" organs a weighing factor of 0.12/13 was used. Dose to organs outside the head and neck area was considered negligible and assumed to be zero. The same assumption was, in study I and II, done for organs estimated to contribute less than 1% to the resulting effective doses: skin and muscle.

Several organs of interest were only partly positioned inside the head and neck area. In these cases, the dose outside the head and neck area were assumed to be zero. The measured organ dose was then multiplied with the fraction of the organ inside the investigated area, in order to obtain the mean organ dose for the entire organ.

In study I and IV the following organ fractions for an adult male were used.
From Cristy, active marrow: cranium 7.6%, mandible 0.8% and cervical vertebrae 3.9%.[13] From the ICRP reference computational phantom: the osteoprogenitor cells (TM50) cranium 16.3%, mandible 0.4%, cervical vertebrae 2.1%; lymphatic nodes 6.3%; muscle 4.2%.[14] The fraction for esophagus was estimated to 10% and for skin to 5%, in the tradition started by Ludlow et al.[15]

In study III the following fractions for an adult male were used.
According to White and Rose, active marrow: cranium 11.8%, mandible 1.3% and cervical vertebrae 3.4%.[16] The distribution of TM50 was assumed to be the same as for active marrow. The fraction for esophagus was estimated to 10%, and for skin, muscle and lymphatic nodes to 5% in the tradition of Ludlow et al.[15]

In study II the following fractions for a 10-year child was used.
From Cristy, active marrow: cranium 11.6%, mandible 1.1% and cervical vertebrae 2.7%. No data on the osteoprogenitor cells were found for the appropriate age group. The fractions for TM50 were estimated by scaling the fractions for an adult male in the ICRP computational phantom with the active marrow ratio between an adult male and a 10-year child reported by Cristy. The resulting TM50 fractions were: cranium 24.9%, mandible 0.6%, cervical vertebrae 1.5%. The lymphatic node distribution for the adult male in the ICRP computational phantom was used: 6.3%.[14] The esophagus fraction was estimated at 10%

In study I, II and IV the dose to ICRU four-component soft tissue was used for all organs. Mass energy-absorption coefficient ratios from air kerma free in air to dose to water, and then to ICRU four-component soft tissue, were taken from the AAPM protocol for 40–300 kV x-ray beam dosimetry.[11] In study III air kerma was used for all organs of interest. In study I and II back-scatter factors were taken from the AAPM protocol, and in study III and IV the backscatter was measured as part of the detector calibration.

In study I, dose enhancement factors (relating dose at CPE to dose under realistic electron contribution) were calculated for the skeletal dosimetry, based on Monte Carlo simulations

published by Johnson et al.[12] For the Promax 3D CBCT (HVL 8.0 mm Al) this resulted in the following factors for active marrow: cranium 1.216, mandible 1.017, cervical vertebrae 1.113; and the following factors for TM50: cranium 1.727, mandible 1.796, cervical vertebrae 1.736. For the Lightspeed VCT MDCT (HVL 6.4 mm Al) this resulted in the following factors for active marrow: cranium 1.192, mandible 1.014, cervical vertebrae 1.102; and the following factors for TM50: cranium 1.671, mandible 1.747, cervical vertebrae 1.679.

3.3 RADIATION DETECTORS AND CALLIBRATION (STUDY I-IV)

3.3.1 Uncertainty estimates

Table 2 Uncertainty estimates for a single point dosimeter measurement.

Quantity	Fractional uncertainty (k=1)	Combined uncertainty (k=2)	Reference
Uncertainty for point dose measurement.			
Type B			
N_k	1.2%		
Beam quality differences	2.0%		11
Backscatter factor B_{water}	1.5%		11
$P_{stem,air}$	1.0%		11
$[(\bar{\mu}_{en}/\rho)_{air}^{water}]_{air}$	1.5%		11
Simultaneous calibration of several detectors (backscatter)	2.0%		
Field inhomogeneities	2.0%		
$(\bar{\mu}_{en}/\rho)_{water}^{ICRU\ 4-comp\ soft\ tissue}$	1.0%		11
Determining dose at different depths inside phantom	3.0%		11
Energy dependence	2.0%		17,18,19
MOSFET angular dependence	5.0%		20
TLD combined		**11.5%**	
MOSFET combined		**15.2%**	
Type A $(s/\sqrt{N})$			
TLD	negligible		
MOSFET	About 3% to 50%		

The uncertainty in a single measurement is comprised of several elements due to the calibration process and dosimeter properties. Estimated components and combined standard uncertainties are shown in Table 2. The combined fractional uncertainty is calculated according to Equation 2.

$$\frac{\Delta D}{D} = \sqrt{\sum_i \left(\frac{\Delta x_i}{x_i}\right)^2} \qquad (2)$$

The mean organ dose is given by Equation 3, where N is the number of measurement points.

$$H_t = \frac{1}{N}\sum_i^N D_i \quad (3)$$

Not all Type B uncertainties can be assumed to be independent between measurement points. However, even if the assume complete correlation the fractional uncertainty in the mean organ dose is at most equal to the fractional uncertainty in the individual measurement point, assuming negligible type A error (Equation 4).

$$\frac{\Delta H_t}{H_t} \leq \sqrt{\frac{1}{N}\sum_i^N \left(\frac{\Delta D_i}{D_i}\right)^2} = \frac{\Delta D}{D} \quad (4)$$

This would be an overestimation of the uncertainty, since not all of the type B errors are correlated. Though, even with this overestimation other, independent, errors will completely dominate the uncertainty of the mean organ dose. In the MOSFET measurements, we have large type B errors due to low detector signal, especially in study III.

However, in both the TLD and MOSFET the dominant uncertainties of the mean organ doses relate to how well the measured point doses are representative of the organ doses. These uncertainties arise from difficulties in accurately estimating the organ shape, and evenly covering the organ mass with measurement points. For organs completely inside the x-ray field these uncertainties are of manageable size. For organs partially or completely outside the x-ray field, these uncertainties become worse, due to significant dose gradients.[21] This problem is further exacerbated if the number of measurement points is low in regards to the organ size.

The magnitude of these uncertainties is hard to accurately estimate. To represent the uncertainty at an adequate number of measurement points, the estimates by Martin are used for organs inside and outside the x-ray field.[21] For the MOSFET measurement additional uncertainty factors were included, due to the low number of measurement points (20). These were estimated based on results by Pauwels et al., who compared organ dose measurements in the head-and-neck area with 150 measurement points and 24 measurement points.[22] The estimated combined standard uncertainties in organ dose are shown in Table 3.

TLD measurements with many measurement points have been shown to agree well with MC simulations with voxelized phantoms; Ernst et al. obtained the following standard deviations between organ dose measured from 73 TLD measurement points and MC simulated organ dose: 3.7% at 4×4 cm FOV, 3.4% at 8×5 cm FOV and 5.1% at 14×10 cm FOV.[23] The 61 measurement points inside an adult phantom in study I and 34 inside a 10-year child phantom in study II are assumed to be sufficient, and no additional uncertainty estimate is employed.

Table 3 Uncertainty in mean organ dose, assuming a 5.7% correlated error for TLD and film, and 7.6% correlated error for MOSFET (k=1).

Quantity	Fractional uncertainty (k=1)	Combined uncertainty (k=2)	Reference
Uncertainties in mean organ dose.			
Film scanner	2.0%		[24]
Positioning, measurement points and organs shape: almost completely inside x-ray field	15%	**32%**	[21]
Positioning, measurement points and organs shape: partly or completely outside x-ray field	40%	**81%**	[21]
Additional error: Few measurement points, study III (panoramic)	60%	**145%**	
Additional error: Few measurement points, study IV (CBCT)	25%	**95%**	

Due to the small x-ray field size, all organs are considered partially or completely outside the x-ray field. The uncertainty in effective dose calculated according to equation 5. For MOSFET measurements the type B error was determined and included in the uncertainty calculation.

$$\Delta E = \sqrt{\sum_t^{\text{organs}} \left(H_t \cdot w_t \cdot \frac{\Delta H_t}{H_t} \right)^2} \qquad (5)$$

3.3.2 Thermoluminescent dosimeters

LiF:Mg TLD-100 equivalent dosimeters were used in study I and II. The dosimeters were cross-calibrated at an accredited dosimetry laboratory in accordance with the in-air method from the AAPM protocol for 40–300 kV x-ray beam dosimetry, against an ion chamber calibrated at the Swedish secondary standard laboratory.[11]

The lowest signal was about 10 times higher than the background, making the type B errors negligible.

3.3.3 Dosimetric film

Gafchromic-QR2 dosimetric film (International Specialty Products, Wayne, USA) was used in study II. The film was calibrated in the same manner as the TLDs. However, due to the non-linear dose response of film, signal-to-dose calibration curves were determined for each x-ray spectrum. This calibration was applied on a pixel by pixel basis on the scanned film.

3.3.4 MOSFET dosimeters

A TN-RD-70-W20 MOSFET device (Best Medical Canada, Ottawa, Canada) was used during study II and IV. The calibration process and characterisation of dosimetric properties have been described in-depth in a series of articles.[18,20,25] The MOSFET detectors were cross calibrated against an ion chamber calibrated at the Finnish secondary standard laboratory. The cross-calibration was performed device with an x-ray device with 2.5 mm Al total

filtration. At these conditions, the energy dependence was confirmed to be very small.[18] The MOSFET detectors have a noticeable angular dependence free in air: down to 67% dose response at the extreme for axial rotations, with a standard deviation from the mean dose responce of 12%.[20] In-phantom measurements showed a much lower angular dependence: 5% standard deviation and 85% as the lowest dose response. The influence of the angular dependence was reduced by correcting the detector signal with the mean dose response over the irradiated angles.

In study IV each exposure was repeated six times, with readout after each exposure. In study III each exposure was repeated 10 times, with readout after each exposure.

3.3.5 DAP measurements

During all measurements, independent DAP measurements were obtained using external DAP-meters mounted at the x-ray tube side and corrected for temperature and pressure. In cases where effective dose was determined at several exposure levels but the x-ray spectra, FOV and positioning were kept constant (i.e. study I and IV), organ dose measurements were only performed at one exposure level. The effective dose at the other exposure levels was calculated by scaling the effective dose with the DAP-ratio between the exposure in question and the organ dose measurement.

3.4 OPTIMIZATION OF DOSE AND IMAGE QUALITY (STUDY I & III)

3.4.1 Exposure level (study I)

In order to optimize the dose/image quality of the CBCT and MDCT examination, an observer study was conducted at several dose levels. Images were acquired at five different dose levels for both x-ray devices, by changing the tube current setting. All other parameters were kept constant. For the CBCT the tube current settings were between 4 mA and 12 mA in intervals of 2 mA. Pre-optimization tube current settings were 12 mA for the CBCT, the highest possible setting. For the MDCT the tube current settings were between 50 mA and 90 mA in steps of 10 mA, with the pre-optimization setting being 73 mA.

The observers consisted of four specialists in dento-maxillofacial radiology with experience of both CBCT and MDCT images. Four different image quality were defined: how well the intra-articulate joint space could be defined, the definition of the cortical bone, the definition of the trabecular bone and the subjective noise level. Each observer also rated their overall impression of the image quality.

Each criterion was rated on a scale from 1-3, where 1 = unacceptable, 2 = acceptable, 3 = excellent. The optimized exposure level was defined as the lowest dose where all four observers rated all four criteria as at least acceptable.

3.4.2 Image size (study III)

Reducing the size of the imaged and therefore irradiated area is one of the most effective ways of reducing the dose. This is often applied in dental CBCT but not extensively used in panoramic radiology.[26] In most cases a smaller image size is available for children,[27] however, some panoramic devices, such as the Promax 2D, have more options to restrict the image size further. In the case of Promax 2D the user has the option to collimate the x-ray field further and remove several image segments to customize the image size. Ten possible collimations were investigated (Figure 9).

To investigate the clinical applicability of reduced image size in panoramic radiographs a retrospective study was performed on 252 patient cases. All referrals to our university clinic during a three-month period with patients aged 18 and above were included, if the patient had a panoramic image taken during this three-month period or within one year prior.

Based on the diagnostic question in the referral, one specialist in dento-maxillofacial radiology (DB) categorized each case in accordance with the smallest suitable collimation. Each case was also categorized according to the clinical indication for the referral.

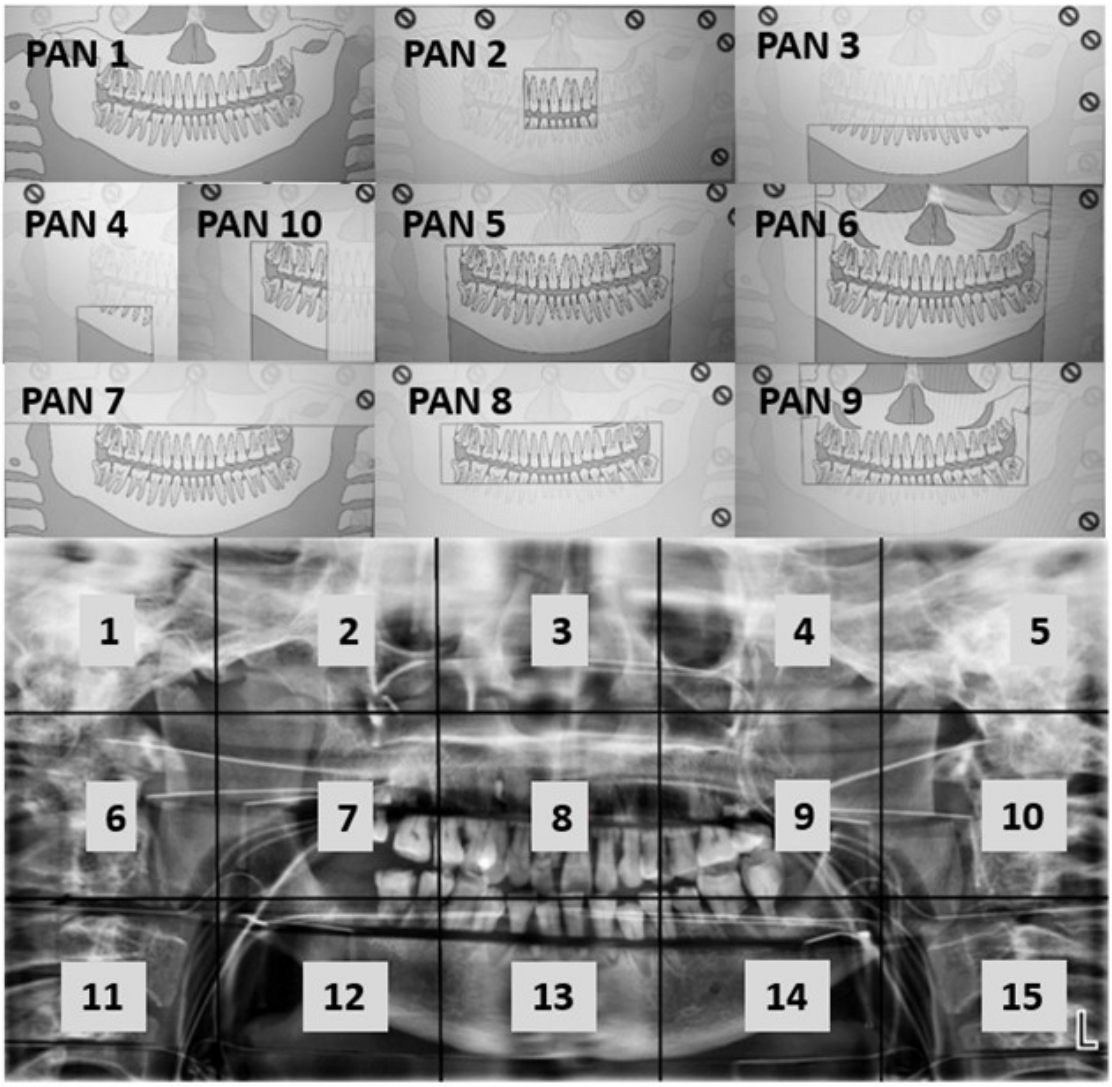

Figure 9 The 10 different collimations investigated in the study and a panoramic radiograph of the phantom with MOSFET and lead cables visible. The numbered squares show the position of the segments which may be removed. Image from study III.

4 STUDY RESULTS AND DISCUSSIONS

4.1 STUDY I

4.1.1 Results

4.1.1.1 Dose optimization

The optimized tube current level for the CBCT was 6mA, half of the pre-optimization level. For the MDCT the optimized mA level was 80mA, close to the pre-optimization level of 73 mA. Figure 10 shows the distribution of the observer ratings on overall image quality at different exposure levels.

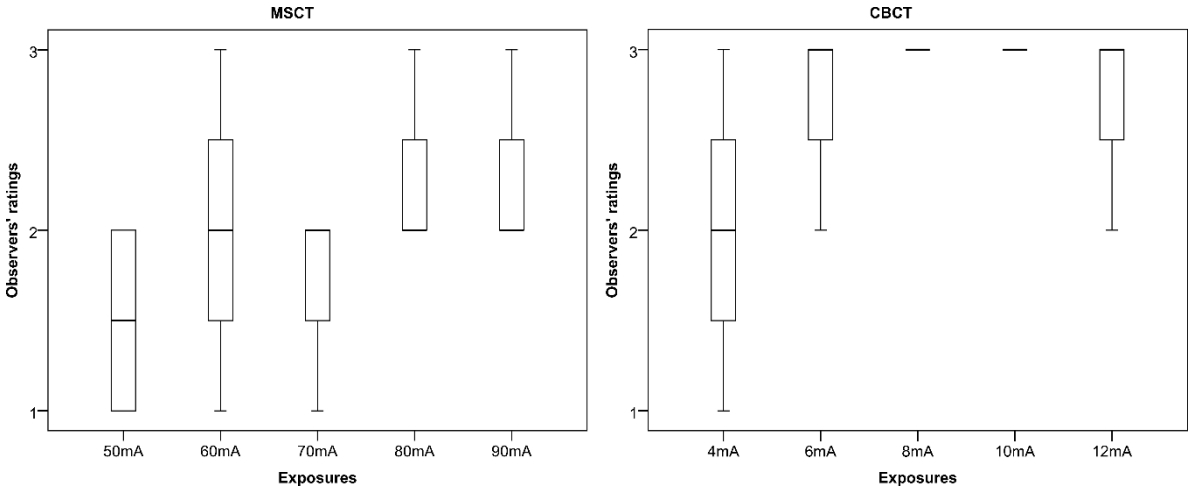

Figure 10 Observer rating of overall image quality (from study I). 1 = unacceptable, 2 = acceptable, 3 = excellent

4.1.1.2 Dosimetry

Pre-optimization, a bilateral CBCT-examination of the TMJ resulted in about 60% higher effective dose compared to the MDCT (Table 4). After optimization, this had been reversed, with MDCT resulting in a 35% higher effective dose than the bilateral CBCT examination (Table 5). The relative contribution to effective dose from the different organs is shown in Figure 11 and Figure 12. The expanded (k=2) relative uncertainty in the effective dose was 35% for CBCT and 34% for MDCT. The difference in effective dose for the optimized examinations was not significant at the 95% confidence level.

Table 4 Pre-optimization effective dose ± standard uncertainty (k=1), dose index and HVL for bilateral and unilateral TMJ-examinations.

Device and examination	Scan length/FOV	Effective dose [µSv]	DAP [Gycm^2]	CTDIvol [mGy]	DLP [mGycm]	HVL [mm Al]
Lightspeed VCT bilateral TMJ	3 cm	113 ± 19	-	7.42	38.2	6.4
Promax 3D unilateral TMJ	4 × 5 cm	92 ± 16	0.606	-	-	8.0
Promax 3D bilateral TMJ	4 × 5 cm × 2	184 ± 32	1.21	-	-	8.0

Table 5 Post-optimization effective dose ± standard uncertainty (k=1), dose index and HVL for bilateral and unilateral TMJ-examinations

Device and examination	Scan length/FOV	Effective dose [µSv]	DAP [Gycm^2]	CTDIvol [mGy]	DLP [mGycm]	HVL [mm Al]
Lightspeed VCT bilateral TMJ	3 cm	124 ± 21	-	8.13	41.9	6.4
Promax 3D unilateral TMJ	4 × 5 cm	46 ± 8	0.303	-	-	8.0
Promax 3D bilateral TMJ	4 × 5 cm × 2	92 ± 16	0.606	-	-	8.0

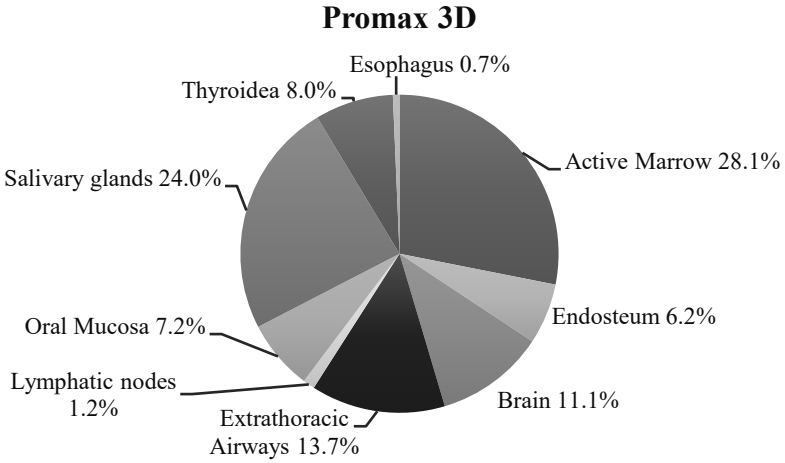

Figure 11 Relative contribution to the resulting effective dose from different organs for the Promax 3D examinations.

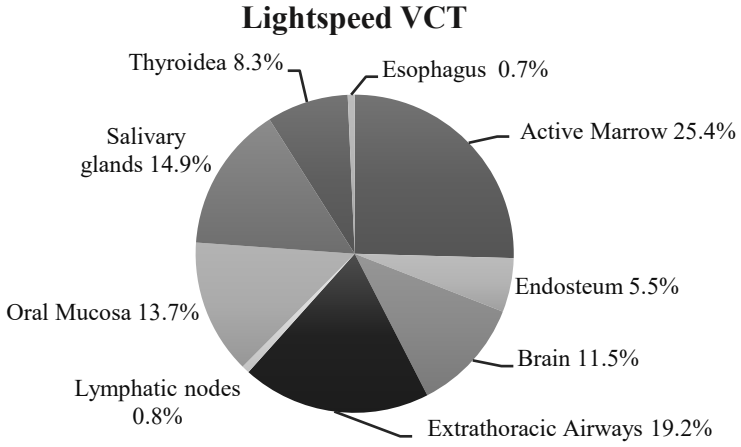

Figure 12 Relative contribution to the resulting effective dose from different organs for the Lightspeed VCT examination.

4.1.2 Discussion

4.1.2.1 Dose optimization

The dose optimization performed in this study is relatively basic, only using a single phantom and only altering a single parameter, tube current. The optimization could be improved in several ways such as using patient cases or investigating other parameters such as tube voltage. The main reasons for the study design were, in the case of avoiding patient examinations, ethical considerations in exposing patients to multiple unnecessary examinations and, in the case of only investigating the tube current, to allow the effective dose to be easily scalable from the TLD measurements.

The resulting optimization method is a pragmatic and relatively quick method that could be used routinely to optimize new equipment for different examinations and diagnostic tasks. The lack of patient images would necessitate a follow-up period, in which the clinical cases are evaluated to ensure that the optimized exposure settings are appropriate under clinical conditions. The resulting decrease in dose from the CBCT examination, down to 50% from the factory preset, highlights the importance of optimization by the user as well as the importance for the manufacturer to allow the user to manually adjust exposure settings. Both these aspects and their importance have been emphasized in the SEDENTEXCT guidelines.[28]

Regarding optimization of the tube voltage, user optimization of this settings was not considered as important as tube current optimization. In dentomaxillofacial CBCT higher kV are generally considered to give better image quality per x-ray dose. E.g. Pauwels et al. have shown an improvement in CNR with the increase of kV for a 3.1 mm al total filtration CBCT device, with the highest CNR obtained at the maximum setting of 90 kV (3.2 mm Al HVL).[29] Lofthag-Hansen et al. have also shown a general tendency of higher tube voltage providing more dose efficient CBCT examinations.[30] However, the Planmeca CBCT devices use higher energy then most x-ray devices, due to the very thick 0.5 mm Cu filtration. We used the highest tube voltage setting 90 kV, resulting in an HVL of about 8.0 mm Al. It would be of future interest to investigate if higher kV is advantageous even at these strongly filtrated x-ray beams.

4.1.2.2 Comparison between CBCT and MDCT

At optimized exposure levels, the Lightspeed VCT MDCT examination resulted in 35% higher effective dose compared to a bilateral Promax 3D CBCT examination. This small difference was not statistically significant. Looking at the literature there are few published doses from TMJ examinations with CBCT. In 2011 Librizzi et al. reported an effective dose 550µSv for a bilateral TMJ examination with a CB MercuRay (Hitachi Medical, Twinsburgh, USA) and either one 9-inch FOV or two 6-inch FOVs.[31] In 2013 Lukat et al. reported an effective dose of 220µSv for an examination with a CB MercuRay and 9-inch FOV, and an effective dose of 20µSv for two 5.0 × 3.7 cm FOV with a Kodak 9000 3D (Carestream, Rochester, NY).[32] I am not aware of any other published studies on the radiation dose from MDCT of the TMJ.

The variation in effective dose from CBCT in the literature is several times larger than the difference we saw between Promax 3D and Lightspeed VCT. A major part of this difference comes from the different FOV sizes available, with not all CBCT models offering suitable FOVs for TMJ diagnostics. It's also worth noticing that two authors reported on the same CBCT model with drastically different radiation dose due to different exposure protocol employed. It is not clear if this is due to user optimization of the exposure protocols, or if the factory preset changed overtime.

4.1.2.3 Bone dosimetry

It is rare to properly correct for the interface effects in bone dosimetry. Generally, one of two alternatives are used: either no corrections are applied for either tissue, or no correction is applied to active marrow but the dose to the osteoprogenitor cells is multiplied with the mass-energy absorption ratio for cortical bone, thus calculating the dose to a solid slab of mineralized bone.

The size of the dose enhancement factors increases with energy and varies between different bones. Thus, the factors will vary with different examination areas and x-ray devices. Cranium has the highest factors of all bones and contributes a large part of the effective dose for head examinations. In the current study, active marrow inside the cranium contributed the most to effective dose of all organs: 21% and 23% for Promax 3D and Lightspeed VCT respectively. This percentage will be lower for dentoalveolar examinations but still major; Pauwels et al. reported a mean contribution of 14% from active marrow for small, medium and large FOV CBCT examinations, with no dose enhancement correction.[22]

In study I the corrections resulted in a 19% and 16% increase in estimated active marrow dose for Promax 3D and Lightspeed VCT respectively, resulting in a 4.7% and 3.8% increase in effective dose. For TM50 the corrections resulted in an 75% dose increase for Promax 3D and 67% dose increase for Lightspeed VCT, resulting in an increased effective dose by 2.8% and 2.3% respectively. The total effect on effective dose from both active marrow and TM dose was 7.5% for Promax3D and 6.1% for lightspeed VCT.

If the mass-energy absorption ratio for cortical bone had been used for TM50 instead, this would have resulted in an increased organ dose of 230% and an 8.8% increase in effective dose for Promax3D and an increased organ dose and effective dose by 270% and 9.3% respectively for Lightspeed VCT.

Even in a reasonable worst-case scenario of 8% systematic underestimation of the effective dose, this can be considered relatively small compared to the uncertainties involved in determining the effective dose from measurements. Studies can be compared in terms of effective dose regardless of the bone dosimetry methods employed, but the differences should be taken into account when comparing individual organ doses.

4.2 STUDY II

4.2.1 Results

The results for each individual image are shown in Table 6. A standard 2D examination could vary from a unilateral examination comprised of two periapical images with different projections up to a bilateral examination using three periapical images and a panoramic image. In the first case this would result in a combined effective dose of 1.2 µSv and in the latter case in 6.0 µSv. Compared to the lowest 2D examination dose a Newtom 5G examination would result in 140 times higher effective dose, and a Promax3D examination in 70 times higher dose. Compared to the highest 2D examination dose a Newtom 5G examination would result in about 30 times higher effective dose, and a Promax3D examination would result in about 15 times higher effective dose.

Table 6 Resulting effective doses with combined standard uncertainties (k=1).

Device (Projection)	Modality	Dosimeter	Image size / FOV [cm]	Effective dose [µSv]	DAP [mGycm^2]	HVL [mm Al]
Promax 3D	CBCT	TLD	4 × 5	88 ± 15	510	8.0
Newtom 5G	CBCT	TLD	6 × 6	172 ± 31	1080	4.4
Newtom 5G	CBCT	Film	6 × 6	166 ± 29	1080	4.4
Promax 2D	Panoramic	Film	19.2 × 9.2	4.1 ± 0.8	21.9	2.9
Prostyle (Periapical lateral)	Intraoral	Film	4.5 × 5.5	0.6 ± 0.1	7.42	2.1
Prostyle (Periapical central)	Intraoral	Film	4.5 × 5.5	0.7 ± 0.2	7.42	2.1

4.2.2 Discussion

Marcu et al. have investigated the effective dose from pediatric examinations with a CBCT device in the Promax3D family.[33] They employed MC simulations using voxelized pediatric 5- and 8-year phantoms. For a maxillary canine examination on the 8-year phantom, using 4.2 x 5.5 cm FOV, 96 kV and 96 mAs, they obtained an effective dose of 125 µSv. In order to compare with our 90 kV examination, the difference in radiation output were estimated by simulating the different x-ray spectra in the SpekCalc software by Gavin Poludniowski.[34,35] Our results, scaled to 96kV, 96 mAs and the slightly larger FOV, would correspond to about 113 µSv. This agrees with the results by Marcu et al. within one standard uncertainty.

In the present study, no optimization study was conducted before comparing the doses from the different x-ray modalities, bringing additional uncertainties to the result. For CBCT the highest resolution modes were used (0.16 mm for promax3D and 0.125 mm for Newtom 5G) and low noise levels were assumed to be required to accurately identify small resorptions. However, potential for dose reduction has been shown by Hidalgo Rivas et al.[36] They investigated CBCT examinations on maxillary impacted canines to identify resorption and found that their radiation dose could be halved, to about 0.146 Gycm^2, while maintaining a small voxel size of 0.08 mm. This DAP value is noticeably lower compared to the ones employed in study II, Newtom 5G resulted in about seven times higher dose. However, some

of the difference is explained by the smaller FOV of 4 × 4 cm used. Still, assuming an x-ray field of the same size as the nominal FOV, our dose level is about three times higher (2.9 for Promax 3D and 3.3 for Newtom5G).

In reality, we do not have the option to reduce the FOV; the smallest available volume was used for both CBCT devices. On Promax 3D the user can manually set the tube current, but Newtom 5G lack the option to manually set the exposure level. In this case the user is limited to lowering the dose about 30% by reducing the number of acquired image frames (Study IV). This exemplifies that not all CBCT devices are designed to perform the full range of dento-maxillofacial examinations at optimized dose.

If we were to convert the DAP for the Hidalgo Rivas optimized exposure protocol into effective dose, using conversion factors calculated from our results, it would result in between 25 µSv and 22 µSv. This is about 4 to 14 times higher than our complete 2D examinations. While this difference is noticeably smaller than our results, the CBCT dose is still significantly higher. Therefore, the recommendation would be to start with periapical images, and only continue with CBCT images when it is required.

More root resorptions are detected in CBCT examinations compared to 2D examinations.[37–39] However, it is not clear if the increased detection results in significant changes in treatment plans. Some studies show significant differences,[39,40] but some do not.[38,41] Based on results by Christell et al. (investigating 12 patient cases, where only one had their treatment plan significantly changed by CBCT), it might be possible to identify selection criteria for when CBCT is recommended.[42] However, further studies on a larger patient populations are required to determine evidence based selection criteria.

4.3 STUDY III

4.3.1 Results

4.3.1.1 Dosimetry

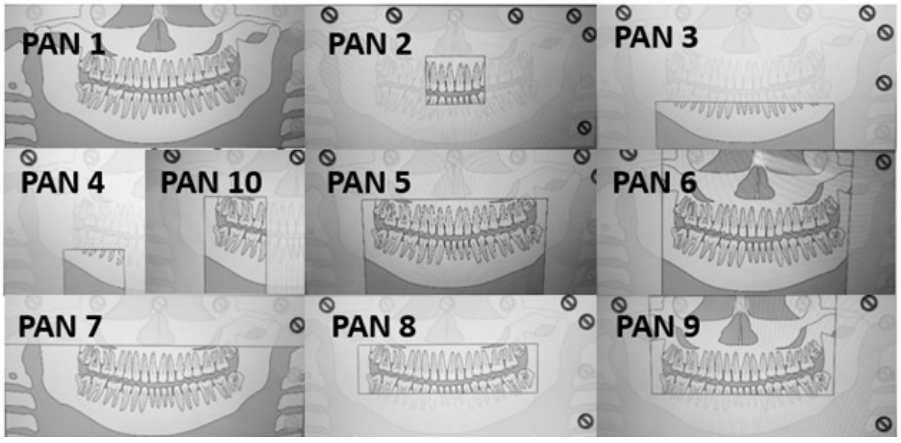

Figure 13 The ten different collimations investigated in the study. Image from study III.

The imaged area of each protocol is illustrated in Figure 13. Effective doses for each protocol and relative dose level compared to a full field panoramic are shown in Table 7.

Table 7 Effective dose results ± standard uncertainty (k=1), relative dose level compared to PAN1, and measured DAP value for each protocol.

Protocol	Effective dose [µSv]	Combined expanded uncertainty k=2	Relative dose (%)	DAP [mGycm^2]
PAN 1	17.6 ± 5.5	63%	100	83
PAN 2	2.3 ± 0.7	60%	13.1	9.2
PAN 3	7.9 ± 2.6	66%	44.9	20
PAN 4	5.0 ± 1.7	69%	28.4	5.9
PAN 5	10.5 ± 3.5	66%	59.7	38
PAN 6	11.7 ± 3.6	62%	66.5	57
PAN 7	16.8 ± 5.4	64%	95.5	56
PAN 8	4.6 ± 1.5	64%	26.1	19
PAN 9	4.5 ± 1.3	61%	25.6	37
PAN 10	5.9 ± 1.9	66%	33.5	11

4.3.1.2 Dose optimization

In 20% of the cases a full field panoramic radiograph was deemed required (Figure 14). Clinical indications generally requiring a full field radiograph in case of trauma, orthodontic/orthognathic treatment and TMJ. Most cases, about 60%, could be performed with PAN5, limiting the view to the teeth and parts of the mandible and maxilla. In some cases, about 7%, PAN10 could be used for imaging of unilateral mandibular molar. Other protocols were rarely deemed suitable and only accounted for about 12% of the cases.

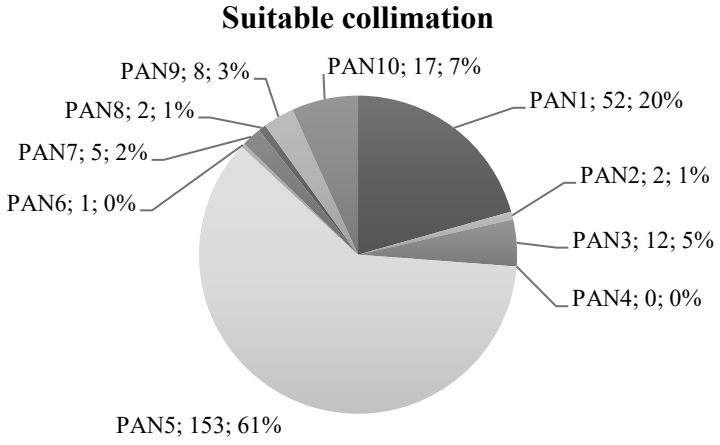

Figure 14 Suitable collimation for each of the 252 patient cases based on the referral. Results presented as protocol; number of cases; percentage of total cases.

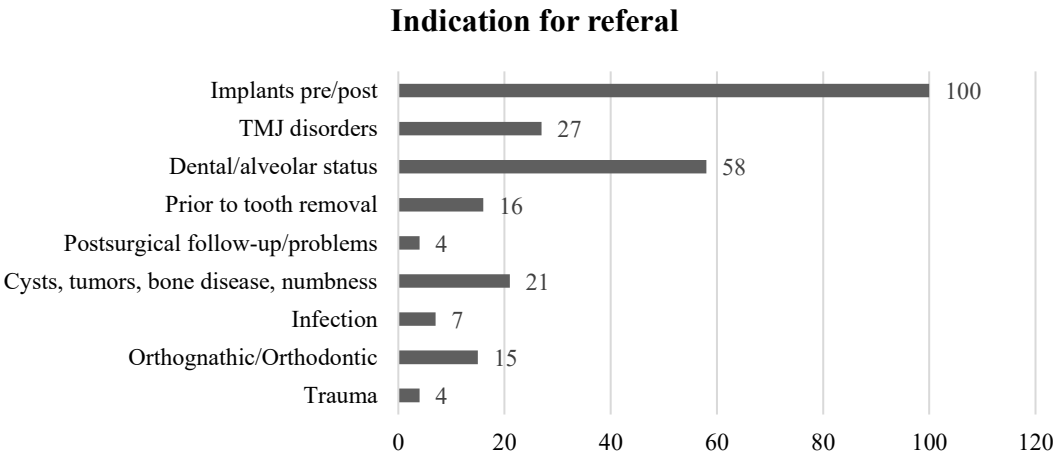

Figure 15 Clinical indication for referral for the 252 patient cases.

Using two collimated protocols, PAN1&5, resulted in a large DAP reduction of about 40% when considering the combined DAP for all patient cases included (Figure 16). Using additional collimated protocols showed little effect, with about 2% reduction in total DAP for each now protocol added from 3 to 5. Additional protocols above 5 showed no discernible effect.

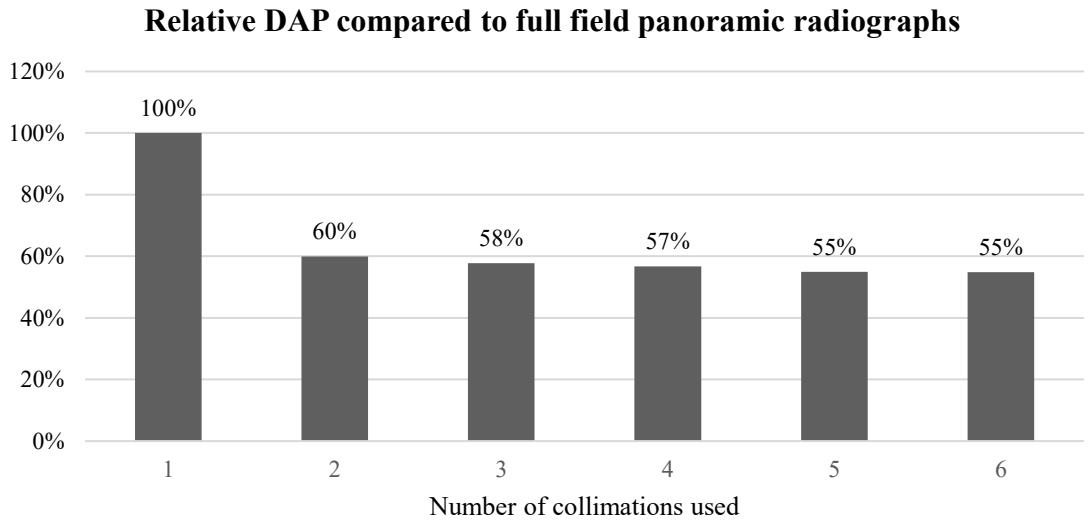

Figure 16 DAP reduction potential with increased number of collimations employed. Number of protocols: 1 PAN1; 2 PAN5&1. 3 PAN5,1&10; 4 PAN5,1,10&3;5 PAN5,1,10,3&9; 6 PAN5,1,10,3,9&7.

4.3.2 Discussion

4.3.2.1 Dosimetry

Organ dose measurements in panoramic x-ray are problematic, and the effects are clearly visible in this study. The choice of MOSFET dosimetry exacerbates these problems and results in high uncertainties. The low detector dose and the relatively low sensitivity of MOSFET compared to TLD, resulting in high Type A uncertainties.[18]

In regard to detector placement, there is a problem with a lack of measurement points in the height of the nasal cavity. This is seen in the very similar results for PAN 1 and 7; PAN 6 and 5; and PAN 8 and 9. These results are explained by no measurement point being located in the phantom slice corresponding to this area.

The low number of measurement points is a major problem in small x-ray fields.[22] Due to the distinctive dose distribution in panoramic x-ray (Figure 17), with it's very small high-dose regions this problem is expected to be even worse than for small field CBCT. The uncertainty introduced by sampling from point measurements in general, and so few measurement points specifically, is very hard to estimate. The uncertainty estimation was based on results for small field CBCT using 24 measurement points versus 150 measurement points published by Pauwels et al., with the assumption that the deviation for panoramic x-ray would have similar uncertainties as the worst case in CBCT.[22] However, it is not obvious that even a 150 measurement point setup would be enough, due to the extreme dose distributions in panoramic x-ray. In general, film dosimetry or Monte Carlo simulation are methods preferred for organ dose measurements for panoramic radiography. Except in cases where effective doses are required, due to comparison with other x-ray modalities or x-ray of other regions, organ dose measurement should generally be avoided in panoramic x-ray. For dose optimization purposes and comparisons within the modality, the dose index (DAP) should be used directly to avoid introducing additional uncertainties.

DAP to E conversion factors for full field panoramic examinations, ranging from 0.087 to 0.131 µSv/mGycm^2, have been published by Loe. et al.[43] In contrast, we obtained a conversion factor of 0.212 µSv/mGycm^2. Loe et. al. used 106 TLDs, likely making their results more reliable than in the current study.

Figure 17 Left, dose distribution in CBCT (Newtom5G), in contrast with dose distribution from panoramic, right.

4.3.2.2 Dose optimization

Using several different collimated protocols may result in decreased patient doses. However, this must be judged against the possible drawback of missing important diagnostic information outside the imaged area. Using a larger field size than in the suitable collimated protocols was not considered justified since there is no indication to expect clinical findings outside this area. However, adding more protocols to clinical routine increases the complexities for the staff and increases the risk of the wrong collimation being chosen by mistake. This might result in patient recalls for additional examination, with additional radiation dose, or worse: the omission of pathology. Therefore, collimated panoramic examination should only be introduced as a clinical routine in cases of noticeable benefit in terms of the collective patient dose.

Due to the uncertainties in determining the effective dose, DAP was used to compare the relative dose reduction between different collimated protocols. For the patient cases at our University clinic the use of two different collimations, full field (PAN1) and teeth including parts of the mandible and maxilla (PAN5), are recommended. The main reason for this is the rarity of patient cases in which other collimation protocols were deemed suitable. However, not all clinics have the same patient case profile, and the benefit should be judged for the common clinical indication at the specific clinic. E.g. one clinical indication that is likely to be more common in general dental clinics are examinations of mandibular molars. In these clinics, the inclusion of PAN10 in clinical practice might be justified. This would result in about 70% dose reduction for these patients, compared to PAN5.

4.4 STUDY IV

4.4.1 Results

Resulting effective doses from the MOSFET measurements and DAP to E conversion factors are shown in Table 8. Effective doses at all available exposure settings, calculated from independent DAP measurements and the conversion factors mentioned above, are shown in Table 9.

Table 8 Results for the MOSFET measurements of effective dose for each combination of position, resolution and FOV, using Regular scan mode. DAP to E conversion factors are calculated from the measured DAP and effective dose. Uncertainties for effective dose and conversion factor presented with k=1.

Positioning	FOV [cm]	Voxel size [mm]	DAP [Gycm^2]	Effective dose [µSv]	Conversion factor [µSv/Gycm^2]
Maxilla front	6 × 6	0.15 (HiRes)	0.898	85.0 ± 18	95 ± 20
Mandible	6 × 6	0.15 (HiRes)	0.967	116 ± 25	120 ± 26
Premolar	6 × 6	0.15 (HiRes)	1.13	135 ± 30	119 ± 26
Dentoalveolar	8 × 8	0.15 (HiRes)	1.77	209 ± 44	118 ± 25
Dentoalveolar	8 × 8	0.30 (StdRes)	0.627	69.7 ± 15	111 ± 23
TMJ/Ear	15 × 5	0.15 (HiRes)	2.28	185 ± 41	81 ± 18

For dental examinations, the lowest effective dose was 45 µSv for 8 × 8 cm FOV, standard resolution and *Eco scan* mode. The highest effective dose was 259 µSv for 8 × 8 cm FOV, high resolution and *Enhanced* scan mode. TMJ protocols ranged from 107 to 217 µSv depending on scan mode. The use of high-resolution mode resulted in about 2.9 times higher dose compared to standard resolution. The reduced view sampling of the *Eco scan* mode resulted in about 30% lower dose, while increased view sampling, *Enhanced* scan mode, resulted in about 40% higher dose compared to *Regular* scan mode.

Table 9 Effective dose (± combined uncertainty k=1), calculated from DAP to E conversion factors, for all available exposure settings.

FOV & Resolution mode	Position	Scan mode	Frames	DAP [Gycm^2]	Effective dose [µSv]
6 × 6 [HiRes]	Maxilla front	Eco	248	0.709	67 ± 14
6 × 6 [HiRes]	Maxilla front	Regular	417	0.973	92 ± 19
6 × 6 [HiRes]	Maxilla front	Enhanced	501	1.43	136 ± 29
6 × 6 [HiRes]	Mandible	Eco	248	0.737	89 ± 19
6 × 6 [HiRes]	Mandible	Regular	417	1.02	122 ± 27
6 × 6 [HiRes]	Mandible	Enhanced	501	1.49	179 ± 39
6 × 6 [HiRes]	Premolar	Eco	248	0.785	94 ± 20
6 × 6 [HiRes]	Premolar	Regular	417	1.10	131 ± 28
6 × 6 [HiRes]	Premolar	Enhanced	501	1.59	189 ± 40
8 × 8 [HiRes]	Dentoalveolar	Eco	248	1.15	128 ± 27
8 × 8 [HiRes]	Dentoalveolar	Regular	372	1.73	193 ± 41
8 × 8 [HiRes]	Dentoalveolar	Enhanced	501	2.33	259 ± 55
8 × 8 [StdRes]	Dentoalveolar	Eco	249	0.379	45 ± 9
8 × 8 [StdRes]	Dentoalveolar	Regular	374	0.571	67 ± 14
8 × 8 [StdRes]	Dentoalveolar	Regular +boosted	374	0.915	108 ± 22
8 × 8 [StdRes]	Dentoalveolar	Enhanced	460	0.757	89 ± 18
8 × 8 [StdRes]	Dentoalveolar	Enhanced +boosted	460	1.21	143 ± 30
15 × 5 [HiRes]	TMJ/Ear	Eco	226	1.32	107 ± 24
15 × 5 [HiRes]	TMJ/Ear	Regular	373	1.96	159 ± 35
15 × 5 [HiRes]	TMJ/Ear	Enhanced	485	2.68	217 ± 48

4.4.2 Discussion

The DAP to E conversion factors determined showed little variation, with the exception being the TMJ examination and, to a lesser extent, the examination of the anterior maxilla. The different DAP to E conversion factor for TMJ examination compared to conversion factors for dental examinations is expected, considering the different irradiated regions. Therefore, for increased accuracy, specific conversion factors should be used for CBCT examinations of the TMJ or inner ear.

There are two additional explanations for the different DAP to E conversion factor for anterior maxilla compared to other dental programs: a lack of measurement points and the volume extending outside the patient. As noted in study III, there is a lack of measurement points inside the cranial half of the maxilla. This may lead to an underestimation of the effective dose when the volume is centered in the maxilla. Secondly, when more of the

volume extends outside the patient, more radiation will miss the patient and not contribute to the effective dose. Out of these two reasons, the volume extending outside the patient is real and ought to be accounted for in the conversion factor, while the lack of measurement points in the maxilla is a measurement error. Due to the uncertainties in the measurement method, it cannot be determined if specific conversion factors for the anterior maxilla would improve the accuracy when estimating effective dose from DAP measurements.

Stratis et al. have determined effective doses for Newtom 5G examinations of the temporal bone through MC simulation using the ICRP reference adult male phantom.[44] Their 15 × 5 cm FOV examination, analogous to our TMJ/ear examination, resulted in an effective dose of 220 µSv, compared to our results of 185 and 159 µSv. Stratis et al. did not present DAP values but used 143 mAs resulting in 1.54 µSv per mAs, compared to our 101 mAs for 185 µSv resulting in 1.83 µSv per mAs. Our results agreed with Stratis et al. within one standard uncertainty. However, using µSv per mAs to compare the studies does not account for potential individual variations in radiation output and x-ray field size between different Newtom 5G devices.

Nardi et al. have determined effective doses for Newtom 5G though TLD measurements inside an Alderson Rando phantom.[45] For a dentoalveolar examination with 8 × 8 cm FOV high-resolution and enhanced scan mode they got an effective dose of 565 µSv and 1.01 $Gycm^2$ DAP, resulting in a conversion factor of 560 $\mu Sv/Gycm^2$. For an inner ear protocol with 15 × 5 cm FOV high-resolution and enhanced scan mode they got an effective dose of 361 µSv and 1.84 $Gycm^2$ DAP, resulting in a conversion factor of 200 $\mu Sv/Gycm^2$. These results cannot be considered reliable; the 560 $\mu Sv/Gycm^2$ was significantly higher than all other published results (see section 6.1.2, Table 11), indicating problems with either the CBCT device employed or the dosimetric method. The large difference in DAP compared to our results could be explained by the use of nominal DAP displayed by the CBCT device without independent verification measurements. The Newtom 5G DAP calibration method systematically underestimates the DAP, often by 50 to 100%.[a] This underestimation, however, is unlikely to completely explain the resulting conversion factors.

[a] Private communication QR.

5 STUDY CONCLUSIONS

5.1 STUDY I

- No significant difference was seen in the effective dose from optimized TMJ examinations with Promax 3D and Lightspeed VCT.
- The difference in effetive dose from TMJ-examinations with CBCT and MDCT is small compared to the variation within published CBCT doses.
- User optimization of factory preset examination protocols is more important than the choice between CBCT and MDCT.
- The availablily of a suitable FOV is essential for optimized CBCT-examinations. Either a large radius and small height volume for bilateral TMJ or small radius and height for unilateral TMJ.
- Not correcting for bone interface effects leads to an underestimation of the effective dose of up to about 8%. For dentoaveolar examinaitons this underestimation will be less pronounced.

5.2 STUDY II

- The difference in effective dose from CBCT compared to 2D examination ranged from 15 times to 140 times higher.
- Low dose CBCT protocols from the literature resulted in about 4 to 14 times higher dose compared to our 2D examinations.
- It is recommended to start with periaphical radiographs and only continue with CBCT when deemed necesarry.
- Some CBCT models do not allow for optimized examination protocols for the maxilla in children.

5.3 STUDY III

- The inclusion of collimated panoramic radiograhps, limited to the teeth and parts of the mandible and maxilla, in clinical practice in addition to full field panoramic radiographs is recommended. This would lead to a reduction in collective patient dose from panoramic radiographs of about 40% at our university clinic.
- Other collimated protocols were not recommended at our university clinic, due to the low number of applicable patient cases.
- The inclusion of a specific collimation for mandibular molar examinations would be recommended at clinics with a large number of molar examinations, due to a 70% dose reduction compared to a panoramic radiograph of all teeth.
- Due to highly inhomogenius dose distributions, MOSFET-dosimetry is not recommended for panoramic x-ray.

5.4 STUDY IV

- Effective doses for dental and TMJ examinations ranged from 45 μSv to 259 μSv.
- High-resolution mode resulted in about 2.9 times higer dose than corresponing standard-resolution examinations.
- DAP to E conversions factors were: 120 μSv/Gycm^2 for dentoalveolar, mandibular and premolar examinations; 95 μSv/Gycm^2 for examinaitons of the anterior maxilla; 81 μSv/Gycm^2 for examinations of the TMJ or inner ear.

6 GENERAL DISCUSSIONS

6.1 GENERALISATION

Since the introduction of dentomaxillofacial CBCT many studies have determined effective doses through measurements or computer simulations.[46,47] These studies have investigated many different combinations of CBCT models, exposure settings, FOV and position. Of great benefit to the field would be the ability to generalize these results and make them applicable to future CBCT models, thus limiting the need for time consuming investigations. In their review of the field, Al-Okshi et al. failed to generalize effective doses, concluding that most studies lacked the necessary description of relevant parameters to allow comparison between studies.[46] Al-Okshi et al. lists 17 parameters to describe the CBCT examination, dosimeter and phantom.

I would propose a slightly different list of essential parameters required when investigating patient dose, disregarding image quality aspects. In terms of CBCT device and examination: HVL (or tube voltage and filtration), DAP (independently measured), FOV, angle of rotation and positioning. The dosimetric method, calibration and phantom should also be described in sufficient detail to enable the reader to estimate any systematic or random errors.

6.1.1 Uncertainties in patient dosimetry

Based on the estimates employed in this thesis, the standard uncertainty in effective dose for measurements with 20-30 measurement points in adult anthropomorphic phantoms were about 22% for medium FOV (between 5 × 5 cm and 10 × 10 cm) CBCT examinations. MC simulation with geometric phantoms, such as PCXMC, is estimated to have similar uncertainties as above.[48] For small FOV (≤ 5 × 5 cm), if an additional uncertainty in organ dose of 40% is assumed (see section 3.3.1 Uncertainty estimates), the resulting combined uncertainty would be about 25%.

Corresponding measurements with “sufficient” measurement points were assumed a standard uncertainty of about 17%. TLD measurements with 71 measurement points have shown good agreement with MC simulations in voxelized phantoms,[23] while 24 measurement points have been shown insufficient for small FOV.[22] Based on this and practical experience during this thesis, at least 50 measurement points, efficiently used, would be required for the number of measurement points to be deemed sufficient.

The most accurate estimates of effective dose would logically come from MC simulations using the two ICRP reference phantoms. With the use of official reference phantoms, uncertainties due to differences between individual phantoms can be removed. The uncertainty is assumed to be less than for non-reference phantoms and a rough estimate of 12% used.

Table 10 General uncertainty estimates for the effective dose determined though different methods.

Method	Estimated uncertainty in E (k=1)
Point dose measurements. N < 50. Small FOV	25%
MC in geometric phantoms. Small FOV	25%
Point dose measurements. N < 50. Medium FOV	22%
MC in geometric phantoms. Medium FOV	22%
Point dose measurements. N ≥ 50	17%
Film measurements	17%
MC in voxelized phantoms	17%
MC in ICRP reference phantoms	12%

The uncertainties presented in this thesis are realistic estimates based on published results. However, due to a lack of data in the literature, these estimates are themselves uncertain. It would be of future interest to examine the uncertainties closer, preferably through MC simulation in ICRP reference phantoms.

6.1.2 Effective dose conversion factors

The use of DAP to E conversion factors in dentomaxillofacial CBCT have been criticized by some authors, such as Ludlow.[47] One argument put forth against this methodology is that the relation between DAP and effective dose varies with the positioning of the examined area. Therefore, the use of a common DAP to E conversion factor for the entire range dento-maxillofacial examinations is not realistic. However, neither is this necessary.

The parameters causing the variation in DAP to E conversion factors need to be identified, and specific conversion factors determined for each set of parameters. For the concept of conversion factors to be practically applicable, the number of parameters should be kept low to avoid an unmanage amount of different conversion factors.

Some published studies on the patient dose from CBCT presents the DAP values, but many omit this information. Based on the data in the literature, some examples of position specific DAP to E conversion factors are shown in Table 11 and Table 12. Uncertainties are estimated based on Table 10.

Some trends can be inferred from the data, e.g. examinations using a half rotation consistently produce higher DAP to E conversion factors than corresponding examinations using full rotations. While the size of the FOV seem to affect the conversion factors, this variation is relatively minor considering the uncertainties. The x-ray energy may have a large effect on the conversion factor, but there are insufficient data to draw any conclusion.

Table 11 DAP to E conversion factors (C_{DAP}^{E}) for dentoalveolar examinations, calculated from different sources in the literature. Conversion factors followed by * denotes the use of nominal DAP displayed by the device. HVL followed by * denotes a value either taken from other sources or estimated from the tube voltage and filtration.

C_{DAP}^{E} [µSv/ Gycm²]	Uncertainty [k=2]	FOV [cm]	HVL [mm Al]	Angle	Method	MC-phantom/ Nbr. of points	CBCT model	Source
120	± 29	16 × 13	4.2*	360	MC	ICRP	i-Cat Next Gen	Morant et al.[49]
130	± 31	16 × 13	4.2*	180	MC	ICRP	i-Cat Next Gen	Morant et al.
120	± 29	16 × 11	4.2*	360	MC	ICRP	i-Cat Next Gen	Morant et al.
140	± 34	16 × 11	4.2*	180	MC	ICRP	i-Cat Next Gen	Morant et al.
130	± 31	16 × 10	4.2*	360	MC	ICRP	i-Cat Next Gen	Morant et al.
140	± 34	16 × 10	4.2*	180	MC	ICRP	i-Cat Next Gen	Morant et al.
130	± 31	16 × 8	4.2*	360	MC	ICRP	i-Cat Next Gen	Morant et al.
150	± 36	16 × 8	4.2*	180	MC	ICRP	i-Cat Next Gen	Morant et al.
140	± 34	8 × 8	4.2*	360	MC	ICRP	i-Cat Next Gen	Morant et al.
180	± 43	8 × 8	4.2*	180	MC	ICRP	i-Cat Next Gen	Morant et al.
120	± 52	8 × 8	4.4	360	MOSFET	20	Newtom 5G	Study III
110	± 49	8 × 8	4.4	360	MOSFET	20	Newtom 5G	Study III
560*	± 246	8 × 8	4.4*	360	TLD	33	Newtom 5G	Nardi et al.[45]
460*	± 202	12 × 8	4.4*	360	TLD	33	Newtom 5G	Nardi et al.
270	± 117	8 × 8	7.7	200	MOSFET	20	Promax3D	Koivisto et al.[48]
230	± 100	8 × 8	7.7	200	MC	Geometric	Promax3D	Koivisto et al.
120*	± 41	14 × 10	3.96	360	TLD	71	Accuitomo 170	Ernst et al.[23]
110*	± 37	14 × 10	3.96	360	MC	Voxelized	Accuitomo 170	Ernst et al.

Table 12 DAP to E conversion factors (C_{DAP}^{E}) for examinations of the mandible, calculated from different sources in the literature. Conversion factors followed by * denotes the use of nominal DAP displayed by the device. HVL followed by * denotes a value either taken from other sources or estimated from the tube voltage and filtration.

C_{DAP}^{E} [µSv/ Gycm²]	Uncer-tainty [k=2]	FOV [cm]	HVL [mm Al]	Angle	Method	MC-phantom/ Nbr. of points	CBCT model	Source
64	± 28	15.4 × 15.4	2.6*		TLD	22	Alphard VEGA	Kim et al.[50]
63	± 28	15.4 × 15.4	2.6*		TLD	22	Alphard VEGA	Kim et al.
96	± 42	10.2 × 10.2	2.6*		TLD	22	Alphard VEGA	Kim et al.
89	± 39	10.2 × 10.2	2.6*		TLD	22	Alphard VEGA	Kim et al.
140	± 34	16 × 6	4.2*	360	MC	ICRP	i-Cat Next Gen	Morant et al.[49]
160	± 38	16 × 6	4.2*	180	MC	ICRP	i-Cat Next Gen	Morant et al.
120	± 53	6 × 6	4.4	360	MOSFET	20	Newtom 5G	Study III
170	± 75	10 × 8	-	180	MC	Geometric	Veraviewepocs R100	Lindfors et al.[51]
140	± 62	8 × 8	-	360	MC	Geometric	Accuitomo F80	Lindfors et al.

While there are insufficient data in the literature to establish any general conversion factors, the concept of DAP to E conversion factors seem promising. Future studies should investigate the possibility to determine positioning specific conversion factors, and quantify the effect of FOV size, energy and rotation angle. Other possible complications that should be investigated is whether the use of bowtie filters, only present in some CBCT models, significantly affects the DAP to E conversion factors.[52] These investigations would preferably

be performed through MC simulation, due to the combination of high accuracy with the ability to relatively quickly perform a large number of simulations on the effect of adjusting different examination parameters. If successful, this could reduce or eliminate the need for time consuming, model specific, dose studies in dentomaxillofacial CBCT.

7 GENERAL CONCLUSIONS AND FUTURE ASPECTS

- There is a need for more detailed descriptions of the parameters in dose studies to allow for generalization of the results.
- The uncertainties in the determined effective dose are large, especially for methods using few measurement points and small FOV. However, future studies are required to accurately estimate these uncertainties.
- The possibility of determening general DAP to effective dose conversion factors through Monte Carlo simulations should be investigated.

8 ACKNOWLEDGEMENTS

Thanks to all the people supporting this work during the last 8 years! Among them:

My main supervisor Qi-Xie Shi, for her help, support and understanding. My co-supervisors Karin Näsström and Mats Nilsson, for their wise advice. Dr Chrysoula Theodorakou, for generously lending the 10-year phantom in study II. The staff at the odontological x-ray clinic at KI, for all their assistance and their patience with me borrowing their x-ray labs. My great colleges at Karolinska Universitetssjukhuset, X-ray physics, for forgiving me spending time away from the clinic. My friends who assisted with spell and grammar checking the manuscript. My bosses Leif Svensson, Annette Fransson Andreo and Albert Sundvall for providing a research friendly department and enabling my research work.

9 REFERENCES

1. European Commission. Cone Beam CT for Dental and Maxillofacial Radiology: Evidence Based Guidelines, Radiation Protection Publication 172. 2012.

2. Mozzo P, Procacci C, Tacconi A, Tinazzi Martini P, Bergamo Andreis IA. A new volumetric CT machine for dental imaging based on the cone-beam technique: Preliminary results. Eur Radiol. 1998;8(9):1558–64.

3. Feldkamp L a, Davis LC, Kress JW. Practical cone-beam algorithm. J Opt Soc Am A [Internet]. 1984 Jun 1;1(6):612. Available from: https://www.osapublishing.org/abstract.cfm?URI=josaa-1-6-612

4. Kalender WA. Computed Tomography: Fundamentals, System Technology, Image Quality, Applications. 2011.

5. Rehani MM, Gupta R, Bartling S, Sharp GC, Pauwels R, Berris T, et al. Radiological Protection in Cone Beam Computed Tomography (CBCT). ICRP Publication 129. Ann ICRP. 2015;44(1):9–127.

6. Joseph PM, Schulz RA. View sampling requirements in fan beam computed tomography. Med Phys. 1980 Nov;7(6):692–702.

7. Attix FH. Introduction to Radiological Physics and Radiation Dosimetry [Internet]. Wiley; 1986. Available from: https://onlinelibrary.wiley.com/doi/book/10.1002/9783527617135

8. ICRP. The 2007 recommendations of the International Commission on Radiological Protection. ICRP Publication 103. Ann ICRP. 2007;37(2–4):1–332.

9. International Comission on Radiation Units and Measurements. Tissue Substitutes in Radiation Dosimetry and Measurement (Report 44). 1988.

10. Wise KN, Sandborg M, Persliden J, Alm Carlsson G. Sensitivity of coefficients for converting entrance surface dose and kerma- area product to effective dose and energy imparted to the patient. Phys Med Biol. 1999;44(8):1937–54.

11. Ma C-M, Coffey CW, DeWerd L a., Liu C, Nath R, Seltzer SM, et al. AAPM protocol for 40–300 kV x-ray beam dosimetry in radiotherapy and radiobiology. Med Phys. 2001;28(6):868.

12. Johnson PB, Bahadori A a, Eckerman KF, Lee C, Bolch WE. Response functions for computing absorbed dose to skeletal tissues from photon irradiation--an update. Phys Med Biol. 2011 Apr 21;56(8):2347–65.

13. Cristy M. Active bone marrow distribution as a function of age in humans. Phys Med Biol. 1981;26(3):389–400.

14. ICRP. Adult reference computational phantoms. ICRP Publication 110. Ann ICRP. 2009;39(2):1–165.

15. Ludlow JB, Davies-Ludlow LE, Brooks SL, Howerton WB. Dosimetry of 3 CBCT devices for oral and maxillofacial radiology: CB Mercuray, NewTom 3G and i-CAT. Dentomaxillofacial Radiol. 2006 Jul;35(4):219–26.

16. White SC, Rose TC. Absorbed bone marrow dose in certain dental radiographic

techniques. J Am Dent Assoc. 1979 Apr;98(4):553–8.

17. D. Davis S, K. Ross C, N. Mobit P, Van der Zwan L, J. Chase W, R. Shortt K. The response of LiF thermoluminescence dosemeters to photon beams in the energy range from 30 kV X rays to 60Co gamma rays. Radiat Prot Dosimetry. 2003;106(1):33–43.

18. Koivisto JH, Wolff JE, Kiljunen T, Schulze D, Kortesniemi M. Characterization of MOSFET dosimeters for low-dose measurements in maxillofacial anthropomorphic phantoms. J Appl Clin Med Phys. 2015;16(4):266–78.

19. Tomic N, Quintero C, Whiting BR, Aldelaijan S, Bekerat H, Liang L, et al. Characterization of calibration curves and energy dependence GafChromicTM XR-QA2 model based radiochromic film dosimetry system. Med Phys. 2014;41(6):062105.

20. Koivisto J, Kiljunen T, Wolff J, Kortesniemi M. Characterization of MOSFET dosimeter angular dependence in three rotational axes measured free-In-Air and in soft-Tissue equivalent material. J Radiat Res. 2013;54(5):943–9.

21. Martin CJ. Effective dose: How should it be applied to medical exposures? Br J Radiol. 2007 Aug;80(956):639–47.

22. Pauwels R, Beinsberger J, Collaert B, Theodorakou C, Rogers J, Walker A, et al. Effective dose range for dental cone beam computed tomography scanners. Eur J Radiol. 2012 Mar;81(2):267–71.

23. Ernst M, Manser P, Dula K, Volken W, Stampanoni MFM, Fix MK. TLD measurements and Monte carlo calculations of head and neck organ and effective doses for cone beam computed tomography using 3D accuitomo 170. Dentomaxillofacial Radiol. 2017;46(7).

24. Paelinck L, De Neve W, De Wagter C. Precautions and strategies in using a commercial flatbed scanner for radiochromic film dosimetry. Phys Med Biol. 2007;52(1):231–42.

25. Koivisto J, Schulze D, Wolff J, Rottke D. Effective dose assessment in the maxillofacial region using thermoluminescent (TLD) and metal oxide semiconductor field-effect transistor (MOSFET) dosemeters: A comparative study. Dentomaxillofacial Radiol. 2014;43(8):1–6.

26. Esmaeili EP, Waltimo-Siŕen J, Laatikainen T, Haukka J, Ekholm M. Application of segmented dental panoramic tomography among children: Positive effect of continuing education in radiation protection. Dentomaxillofacial Radiol. 2016;45(6).

27. Davis AT, Safi H, Maddison SM. The reduction of dose in paediatric panoramic radiography: The impact of collimator height and programme selection. Dentomaxillofacial Radiol. 2015;44(2).

28. European Commission. Radiation protection 172: Cone beam CT for dental and maxillofacial radiology. Evidence Based Guidelines. 2012.

29. Pauwels R, Silkosessak O, Jacobs R, Bogaerts R, Bosmans H, Panmekiate S. A pragmatic approach to determine the optimal kVp in cone beam CT: Balancing contrast-to-noise ratio and radiation dose. Dentomaxillofacial Radiol. 2014;43(5).

30. Lofthag-Hansen S, Thilander-Klang A, Gröndahl K. Evaluation of subjective image

quality in relation to diagnostic task for cone beam computed tomography with different fields of view. Eur J Radiol. 2011 Nov;80(2):483–8.

31. Librizzi ZT, Tadinada AS, Valiyaparambil J V., Lurie AG, Mallya SM. Cone-beam computed tomography to detect erosions of the temporomandibular joint: Effect of field of view and voxel size on diagnostic efficacy and effective dose. Am J Orthod Dentofac Orthop. 2011 Jul;140(1):e25-30.

32. Lukat TD, Wong JCM, Lam EWN. Small field of view cone beam CT temporomandibular joint imaging dosimetry. Dentomaxillofac Radiol. 2013 Jan;42(10):20130082.

33. Marcu M, Hedesiu M, Salmon B, Pauwels R, Stratis A, Oenning ACC, et al. Estimation of the radiation dose for pediatric CBCT indications: a prospective study on ProMax3D. Int J Paediatr Dent. 2018;28(3):300–9.

34. Poludniowski GG. Calculation of x-ray spectra emerging from an x-ray tube. Part II. X-ray production and filtration in x-ray targets. Med Phys. 2007;34(6):2175–86.

35. Poludniowski GG, Evans PM. Calculation of x-ray spectra emerging from an x-ray tube. Part I. Electron penetration characteristics in x-ray targets. Med Phys. 2007;34(6):2164–74.

36. Hidalgo Rivas JA, Horner K, Thiruvenkatachari B, Davies J, Theodorakou C. Development of a low-dose protocol for cone beam CT examinations of the anterior maxilla in children. Br J Radiol. 2015;88(1054).

37. Alqerban A, Jacobs R, Fieuws S, Willems G. Comparison of two cone beam computed tomographic systems versus panoramic imaging for localization of impacted maxillary canines and detection of root resorption. Eur J Orthod. 2011;33(1):93–102.

38. Alqerban A, Willems G, Bernaerts C, Vangastel J, Politis C, Jacobs R. Orthodontic treatment planning for impacted maxillary canines using conventional records versus 3D CBCT. Eur J Orthod. 2014;36(6):698–707.

39. Botticelli S, Verna C, Cattaneo PM, Heidmann J, Melsen B. Two- versus three-dimensional imaging in subjects with unerupted maxillary canines. Eur J Orthod. 2011;33(4):344–9.

40. Haney E, Gansky SA, Lee JS, Johnson E, Maki K, Miller AJ, et al. Comparative analysis of traditional radiographs and cone-beam computed tomography volumetric images in the diagnosis and treatment planning of maxillary impacted canines. Am J Orthod Dentofac Orthop. 2010;137(5):590–7.

41. Wriedt S, Jaklin J, Al-Nawas B, Wehrbein H. Impacted upper canines: examination and treatment proposal based on 3D versus 2D diagnosis. J Orofac Orthop. 2012;73(1):28–40.

42. Christell H, Birch S, Bondemark L, Horner K, Lindh C. The impact of Cone Beam CT on financial costs and orthodontists' treatment decisions in the management of maxillary canines with eruption disturbance. Eur J Orthod. 2017;

43. Looe HK, Eenboom F, Chofor N, Pfaffenberger A, Steinhoff M, Rühmann A, et al. Conversion coefficients for the estimation of effective doses in intraoral and panoramic dental radiology from dose-area product values. Radiat Prot Dosimetry. 2008;131(3):365–73.

44. Stratis A, Zhang G, Lopez-Rendon X, Politis C, Hermans R, Jacobs R, et al. Two examples of indication specific radiation dose calculations in dental CBCT and Multidetector CT scanners. Phys Medica. 2017;41:71–7.

45. Nardi C, Talamonti C, Pallotta S, Saletti P, Calistri L, Cordopatri C, et al. Head and neck effective dose and quantitative assessment of image quality: A study to compare cone beam CT and multislice spiral CT. Dentomaxillofacial Radiol. 2017;46(7):1–11.

46. Al-Okshi A, Lindh C, Salé H, Gunnarsson M, Rohlin M. Effective dose of cone beam CT (CBCT) of the facial skeleton: a systematic review. Br J Radiol. 2015;88(1045):20140658.

47. Ludlow JB, Timothy R, Walker C, Hunter R, Benavides E, Samuelson DB, et al. Effective dose of dental CBCT - A meta analysis of published data and additional data for nine CBCT units. Dentomaxillofacial Radiol. 2015;44(1).

48. Koivisto J, Kiljunen T, Tapiovaara M, Wolff J, Kortesniemi M. Assessment of radiation exposure in dental cone-beam computerized tomography with the use of metal-oxide semiconductor field-effect transistor (MOSFET) dosimeters and Monte Carlo simulations. Oral Surg Oral Med Oral Pathol Oral Radiol. 2012;114(3):393–400.

49. Morant JJ, Salvad́ M, Herńandez-Giŕon I, Casanovas R, Ortega R, Calzado A. Dosimetry of a cone beam CT device for oral and maxillofacial radiology using Monte Carlo techniques and ICRP adult reference computational phantoms. Dentomaxillofacial Radiol. 2013;42(3):1–9.

50. Kim D-S, Rashsuren O, Kim E-K. Conversion coefficients for the estimation of effective dose in cone-beam CT. Imaging Sci Dent. 2014;44(1):21–9.

51. Lindfors N, Lund H, Johansson H, Ekestubbe A. Influence of patient position and other inherent factors on image quality in two different cone beam computed tomography (CBCT) devices. Eur J Radiol Open. 2017;4(November):132–7.

52. Stratis A, Zhang G, Jacobs R, Bogaerts R, Bosmans H. The growing concern of radiation dose in paediatric dental and maxillofacial CBCT: an easy guide for daily practice. Eur Radiol. 2019;

10 ERRATA

10.1 STUDY III

Table 2 contains incorrect organ doses. The correct mean organ doses should be as follows.

Table 2. Mean absorbed organ doses (μGy) for all panoramic protocols

Organ	PAN 1	PAN 2	PAN 3	PAN 4	PAN 5	PAN 6	PAN 7	PAN 8	PAN 9	PAN 10
Bone Marrow	18	4.9	9.4	2.9	11	10	19	5.4	5.2	4.7
Thyroid	43	8.1	17	22	30	38	50	19	14	19
Esophagus	5.1	0.8	4.0	2.4	2.1	4.1	4.7	1.7	0.8	2.3
Skin	2.4	0.5	0.9	1.1	1.4	1.4	1.3	1.1	0.9	0.7
Bone surface	18	4.9	9.4	2.9	11	10	19	5.4	5.2	4.7
Salivary glands	384	16	274	178	307	325	378	80	65	192
Brain	96	14	17	8.0	19	72	21	15	67	13
Lymphatic nodes	23	2.4	7.7	4.7	12	13	22	5.7	5.1	6.2
Extrathoracic airways	367	42	126	79	200	207	350	95	85	103
Muscle	10	0.8	6.9	4.3	7.7	8.4	10	2.4	1.9	4.6
Oral mucosa	518	58	170	103	278	280	499	131	116	142